

Circadian fluctuation of soluble CD26 dictates the impact of the timing of cord blood transplantation on acute graft-versus-host disease

Received: 12 June 2025

Accepted: 21 January 2026

Published online: 30 January 2026

 Check for updates

Yue Wu^{1,2,3,5}, Yiwen Hou^{1,5}, Dongyao Wang^{1,2,3}, Liang Wang¹, Kaidi Song^{1,2,3}, Guangyu Sun^{1,2,3}, Aijie Huang^{1,2,3}, Meijuan Tu^{1,2,3}, Lu Huang^{1,2,3}, Jialin Zhou¹, Weiwei Wu⁴, Baolin Tang^{1,2,3} ✉, Cheng Zhan¹ ✉ & Xiaoyu Zhu^{1,2,3} ✉

Allogeneic hematopoietic stem cell transplantation (allo-HSCT) is a cornerstone treatment for many malignant and nonmalignant hematological diseases. Our recent research demonstrated that early-day stem cell infusions significantly reduce the incidence and severity of acute graft-versus-host disease (aGVHD) following allo-HSCT using fresh grafts. However, the impact of infusion timing on aGVHD in allo-HSCT with cryopreserved grafts such as unrelated cord blood (UCB) remains unclear. Here, we show that early-morning cord blood infusions significantly reduce aGVHD severity and improve survival. We further found that circadian variations in cytokines, particularly soluble CD26 (sCD26), are correlated with the severity of aGVHD. Inhibiting the enzymatic activity of sCD26 with Sitagliptin significantly mitigated aGVHD and improved survival in late-infused female mice. Our study indicates that scheduling UCB transplantation in the early morning could be a simple and effective prophylactic strategy for aGVHD and that inhibiting sCD26 could be a promising therapeutic approach for late infusions.

Acute graft-versus-host disease (aGVHD) is a formidable complication following allogeneic hematopoietic stem cell transplantation (allo-HSCT)¹. This condition ensues when immunocompetent cells within the graft mount a vigorous immunological assault on the recipient's organs and tissues. Despite remarkable advancements in human leukocyte antigen (HLA) typing, donor selection strategies, conditioning regimens, and the implementation of various potent prophylactic measures, the incidence of aGVHD remains unacceptably high². The quality of life and prognosis of transplant

recipients continue to be limited, posing a significant challenge to the success of allo-HSCT^{3,4}.

In recent years, emerging scientific evidence has illuminated the crucial role of circadian rhythms in orchestrating immune functions and modulating immune responses⁵. The circadian rhythm exerts far-reaching effects across multiple dimensions of immunology⁶, including the circulation patterns of immune cells^{7,8}, the innate and adaptive immune responses^{9,10}, and even the efficacy of tumor immunotherapy^{11–14}. Our recent research identified the circadian

¹Department of Hematology, The First Affiliated Hospital of USTC, National Key Laboratory of Immune Response and Immunotherapy, Division of Life Sciences and Medicine, University of Science and Technology of China, Hefei, China. ²Anhui Provincial Key Laboratory of Blood Research and Applications, Hefei, China. ³Blood and Cell Therapy Institute, Division of Life Sciences and Medicine, University of Science and Technology of China, Hefei, China.

⁴Department of Epidemiology, School of Public Health, Center of Clinical Epidemiology and Evidence-Based Medicine, Shanxi Medical University, Taiyuan, China. ⁵These authors contributed equally: Yue Wu, Yiwen Hou. ✉e-mail: zwcystalbl@163.com; zhancheng@ustc.edu.cn; xiaoyuz@ustc.edu.cn

timing of stem cell infusion as an independent risk factor for the development of aGVHD¹⁵. Specifically, patients who received transplantation before 2:00 pm presented a significantly lower incidence and severity of aGVHD than those who received transplantation after this time point did.

However, several critical questions remain unanswered. First, our previous study included only transplantations with freshly mobilized peripheral blood stem cells (PBSCs) from related donors as grafts. It remains uncertain whether these findings can be generalized to other transplantation modalities, such as unrelated cord blood transplantation (UCBT), which uses cryopreserved grafts. Second, for patients who undergo transplantation before 2:00 pm, it is unclear whether earlier transplantation within this time frame confers additional benefits. For example, thawed cord blood units are commonly infused within a relatively narrow time window (e.g., the morning) because of standardized banking and clinical scheduling protocols. Is there an optimal cutoff time for this type of transplantation that minimizes the risk of aGVHD? Third, we previously showed that the impact of infusion timing on aGVHD is intricately associated with the recipient's postconditioning immune environment, with a particular emphasis on the circadian fluctuations in IL-1 α levels. However, the use of IL-1 α neutralizing antibodies only partially mitigated aGVHD, strongly suggesting the involvement of additional yet unknown factors in this complex pathophysiological process.

Given this background, the present study was designed to address these critical questions. Through an in-depth retrospective analysis of UCBT, we found that patients who underwent UCBT in the early morning experienced significantly reduced aGVHD severity compared with those transplanted later in the day. Mechanistically, we identified soluble CD26/dipeptidyl peptidase 4 (sCD26/DPPIV) as a key player in this process. Moreover, the administration of Sitagliptin, a DPPIV inhibitor approved by the U.S. Food and Drug Administration (FDA) for the treatment of type 2 diabetes mellitus, significantly mitigated aGVHD in mice.

Results

Early morning infusion of cord blood significantly mitigates the severity of aGVHD

To examine the impact of cord blood infusion timing on the development of aGVHD following UCBT, we conducted a historical cohort study. This study included acute leukemia patients who received unrelated thawed single-unit UCBT (SUCBT) for the first time at the Department of Hematology, the First Affiliated Hospital of the University of Science and Technology of China, between January 2014 and December 2020 (Fig. 1a). All patients were in their first or second complete remission before transplantation. The cryopreserved cord blood units were typically delivered from banks one day in advance, and 97% of the patients received transplants before 12 pm. To mitigate bias arising from an excessive imbalance in the number of patients transplanted in the morning versus the afternoon, patients who were infused with cord blood after 12 pm were excluded from this retrospective study.

A total of 434 patients were included in the analysis. The infusion times of this cohort ranged from 8:19 am to 11:56 am, with a median infusion time of 9:40 am (Fig. 1b). Due to the nonnormal distribution of the infusion time, patients were categorized into two groups on the basis of the median infusion time: the "earlier infusion" group (infusion before 9:40 am, $n = 219$) and the "later infusion" group (infusion after 9:40 am, $n = 215$). The clinical characteristics of the two groups were comparable, except for age (Supplementary Data 1).

All patients received a combination of cyclosporine (CsA) and mycophenolate mofetil (MMF) for GVHD prophylaxis. No patients in either group discontinued CsA or MMF during the early posttransplant period because of drug-related toxicity or intolerance. The severity of

aGVHD was diagnosed according to the Mount Sinai Acute GVHD International Consortium (MAGIC) criteria¹⁶. Although no significant differences were observed in the cumulative incidence of grade II-IV aGVHD between the two groups, the earlier infusion group presented a significantly lower cumulative incidence of grade III-IV aGVHD compared to the later infusion group (earlier infusion group vs. later infusion group: grade II-IV aGVHD: 37.0% [95% CI, 30.6-43.4%] vs. 34.0% [95% CI, 27.7-40.3%], $P = 0.416$; grade III-IV aGVHD: 16.0% [95% CI, 11.5-21.2%] vs. 27.9% [95% CI, 22.1-34.0%], $P = 0.004$) (Fig. 1c, d). Specifically, 46 patients had grade II and 35 had grade III-IV aGVHD in the earlier infusion group (Supplementary Data 2), with 34 patients exhibiting skin involvement, 12 with upper gastrointestinal tract (UGI) involvement, 59 with lower gastrointestinal tract (LGI) involvement, and 3 with liver involvement. In contrast, in the later infusion group, more patients developed grade III-IV aGVHD ($n = 60$ patients), with 19 patients exhibiting skin involvement, 8 with UGI involvement, 61 with LGI involvement, and 8 with liver involvement. No significant differences were observed in the cumulative incidence of chronic GVHD (cGVHD) between the two groups (Fig. 1e). These results clearly demonstrated that the earlier infusion group presented significantly lower aGVHD severity than did the later infusion group following UCBT.

We then performed multivariate analysis considering variables including absolute infusion time, patient age, sex, refined disease risk index (DRI-R), complete remission status, donor-recipient sex compatibility, ABO compatibility, high-resolution HLA compatibility, counts of infused total nucleated cells (TNCs), CD34⁺ cell count, and conditioning regimen (irradiation-based vs. Bu-based). Consistent with previous reports^{17,18}, the infused TNC count and HLA compatibility were also independent risk factors for aGVHD in our analysis. Notably, the absolute infusion time was identified as an independent risk factor for grade III-IV aGVHD (HR = 1.37, 95% CI, 1.03-1.83) (Table 1). Our further sensitivity analysis demonstrated that patients grouped by time cutoffs ranging from 9:30 am to 10:00 am consistently exhibited associations with aGVHD severity, thereby reinforcing the robustness of our findings (Supplementary Table 1). However, when the cutoff time was set at 10:00 am, this significant difference disappeared, indicating the presence of a critical threshold effect. Collectively, these results highlight the importance of early morning UCBT in mitigating aGVHD severity.

Other clinical outcomes in UCBT

Importantly, the 3-year transplant-related mortality (TRM) in the earlier infusion group was lower than that in the later infusion group (11.6% [95% CI, 7.8-16.3%] vs. 18.0% [95% CI, 13.1-23.4%], $P = 0.067$) (Fig. 1f). Accordingly, the 3-year overall survival (OS), disease-free survival (DFS), and GVHD-free, relapse-free survival (GRFS) probabilities were greater in the earlier infusion group than in the later infusion group (OS: 78.5% [95% CI, 72.5-83.4%] vs. 68.8% [95% CI, 62.2-74.6%], $P = 0.022$; DFS: 74.9% [95% CI, 68.6-80.1%] vs. 66.0% [95% CI, 59.3-71.9%], $P = 0.050$; GRFS: 60.1% [95% CI, 53.3-66.3%] vs. 45.8% [95% CI, 39.0-52.4%], $P < 0.001$) (Fig. 1g-i). Consistently, multivariate analysis revealed that absolute infusion time was an independent risk factor for 3-year GRFS (HR = 1.36, 95% CI, 1.11-1.66) (Table 1). No significant differences were observed between the two groups in terms of relapse rates, neutrophil engraftment rates, or platelet engraftment rates (Fig. 1j and Supplementary Fig. 1). To further evaluate factors associated with relapse, we performed the multivariate analysis for 3-year relapse using the Fine-Gray model. In this analysis, diagnosis of ALL was the only independent predictor of relapse, whereas R-DRI did not reach statistical significance (HR = 1.43, 95% CI, 0.83-2.45, $P = 0.19$) (Table 1). Although R-DRI is a well-established predictor of post-transplant relapse risk¹⁹, its lack of significance in our model is likely attributable to the relatively homogeneous risk profile of this cohort, in which all patients were transplanted in CR1/CR2 and no

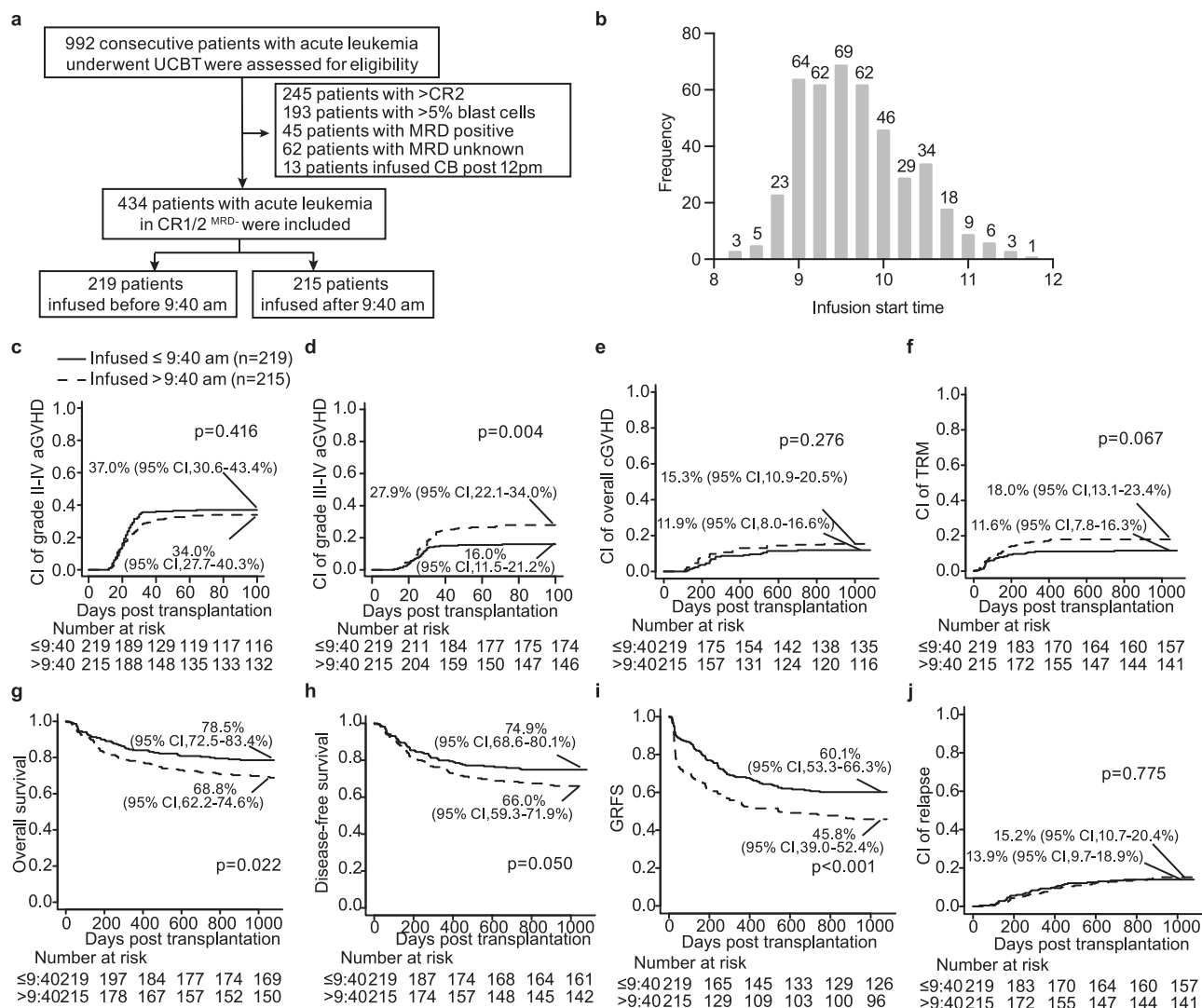


Fig. 1 | Effects of stem cell infusion timing on GVHD incidence and survival in UCBT patients infused prior to 12 pm. **a** Diagram of patients who underwent UCBT. Patients were divided into two groups on the basis of stem cell infusion timing, with a cutoff time of 9:40 am. UCBT, unrelated cord blood transplantation; CR, complete remission; MRD minimal residual disease; CB, cord blood.

b Histogram showing the distribution of stem cell infusion times in the cohort. **c, d** Cumulative incidence (CI) of grade II-IV aGVHD (**c**) ($P=0.416$) and grade III-IV aGVHD (**d**) ($P=0.004$) in the earlier infusion ($\leq 9:40$ am, $n=219$) and later infusion ($> 9:40$ am, $n=215$) groups. The P values are two-sided and reported as exact values. **e** CI of overall chronic GVHD (cGVHD) in the earlier infusion ($\leq 9:40$ am) and

later infusion ($> 9:40$ am) groups ($P=0.276$). The P values are two-sided and reported as exact values. **f** CI of 3-year TRM in the earlier infusion ($\leq 9:40$ am, $n=219$) and later infusion ($> 9:40$ am, $n=215$) groups ($P=0.067$). The P values are two-sided and reported as exact values. **g–i** Probabilities of overall survival (**g**) ($P=0.022$), disease-free survival (**h**) ($P=0.050$), and GRFS (**i**) ($P<0.001$) in the earlier infusion ($\leq 9:40$ am, $n=219$) and later infusion ($> 9:40$ am, $n=215$) groups. **j** CI of 3-year relapse in the earlier infusion ($\leq 9:40$ am, $n=219$) and later infusion ($> 9:40$ am, $n=215$) groups ($P=0.775$). The P values are two-sided and reported as exact values. The data were analyzed by Gray's test (**c–f**, and **j**) and the log-rank test (**g–i**). Source data are provided as a Source Data file.

cases fell into the very high-risk category. These findings support that early morning UCBT scheduling can improve survival outcomes without increasing relapse risk.

Time-of-day variation in sCD26/DPPIV levels is correlated with pretransplant immune milieu

Our prior research revealed that the immune environment of recipients prior to transplantation is a key determinant of donor T-cell responses and the subsequent development of aGVHD¹⁵. To further investigate the underlying mechanism, we analyzed pretransplant serum samples collected from 20 recipients following completion of myeloablative conditioning and prior to cord blood infusion. Ten samples were obtained at 7:00 am \pm 15 min and ten at 11:30 am \pm 15 min (Fig. 2a). Immediately after collection, the samples were stored at 4 °C and processed within 4 h.

We examined the levels of 49 cytokines and chemokines, including soluble CD26 (sCD26, also known as DPPiV), a key molecule that is strongly correlated with T cell activation and immune responses^{20,21}. Notably, sCD26 was the only cytokine that exhibited a statistically significant difference, with its level at 7:00 am being significantly lower than that at 11:30 am (Fig. 2b, c). Moreover, sCD26/DPPIV levels increased further at 4:00 pm than they did in the morning, indicating a distinct diurnal elevation pattern (Fig. 2d). The levels of β -nerve growth factor (β -NGF), interleukin-12 subunit p40 (IL-12 p40), interleukin-1 receptor antagonist (IL-1Ra), macrophage-colony stimulating factor (M-CSF), chemokine (C-C motif) ligand 7 (CCL7), and chemokine (C-C motif) ligand 11 (CCL11) were numerically lower at 7:00 am than at 11:30 am, but the differences were not statistically significant (Fig. 2b, c, and Supplementary Fig. 2). Previous studies have demonstrated that IL-1 α levels in recipients prior to transplantation are significantly lower at

Table 1 | Multivariate analysis of factors associated with aGVHD, relapse and survival in UCBT patients infused prior to 12 pm (n = 434)

Variable	Multivariate analysis		
	HR	95%CI	P
Grade II-IV acute GVHD			
Infused TNCs count	1.10	1.03–1.17	0.002
HLA compatibility	1.38	1.08–1.78	0.012
Grade III-IV acute GVHD			
Infusion time	1.37	1.03–1.83	0.031
Infused TNCs	1.12	1.04–1.20	0.002
HLA compatibility	1.51	1.10–2.06	0.011
3-year TRM			
HLA compatibility	1.73	1.11–2.68	0.015
3-year Relapse			
ALL vs AML	2.69	1.53–4.72	<0.001
3-year OS			
HLA compatibility	1.45	1.07–1.97	0.016
ALL vs AML	1.62	1.11–2.35	0.012
3-year DFS			
ALL vs AML	1.69	1.19–2.41	0.004
3-year GRFS			
Infusion time	1.36	1.11–1.66	0.003

Multivariate analyses of aGVHD, TRM and relapse were performed via the Fine-Gray proportional hazards regression model, whereas OS, DFS, and GRFS were analyzed via the Cox proportional hazards regression model. The infusion times were included as ordinal data. Independent risk factors were identified via the stepwise selection method on the basis of the *P* value. All tests were two-sided, and exact *P* values are reported. No adjustment was made for multiple comparisons. GVHD graft-versus-host disease, TNCs total nucleated cells, HLA human leucocyte antigen, TRM transplant-related mortality, OS overall survival, DFS disease-free survival, GRFS GVHD-free, relapse-free survival.

7:00 am than at 4:00 pm¹⁵. However, in the present study, no significant difference in IL-1 α levels was detected between 7:00 am and 11:30 am, likely due to the relatively short time interval between the two sampling points, suggesting that IL-1 α might not play a critical role in mediating the difference in aGVHD between these two groups.

Moreover, we observed a significant positive correlation between sCD26/DPPIV levels and the levels of multiple proinflammatory cytokines, including IL-1Ra, IL-1 β , and leukemia inhibitory factor (LIF), and a significant negative correlation with the level of IL-18, a cytokine that plays an immunosuppressive role in intestinal immunity²², in patients prior to transplantation (Fig. 2e–h). However, the sCD26/DPPIV levels were not significantly correlated with the IL-1 α levels (*P* = 0.741) (Fig. 2i). These results suggest that pretransplantation sCD26/DPPIV levels exhibit a circadian pattern and may reflect the immune environment of recipients prior to transplantation.

Fluctuation in sCD26/DPPIV is regulated by the circadian rhythm of epithelial cells

Next, we investigated the factors contributing to the variation in sCD26/DPPIV. Circulating sCD26/DPPIV may be released from various cells and tissues, including epithelial cells and lymphocytes²³. Since patients who have undergone myeloablation lack lymphocytes, we reasoned that epithelial cells might be involved. We conducted immunofluorescence staining on intestinal biopsy samples collected from healthy human subjects at different times of the day. We observed a significant difference in CD26/DPPIV expression on intestinal epithelial cells, with notably stronger expression in the evening (Circadian Time18, CT18) and afternoon (CT14) than in the morning (CT10) (Fig. 3a, b). To examine whether changes in CD26/DPPIV expression in epithelial cells influence the levels of circulating sCD26/DPPIV, we cultured primary mouse intestinal epithelial cells

(IECs) and measured sCD26/DPPIV concentrations in the culture supernatant at different time points. *Bmal1* is a core gene that drives the generation and maintenance of the mammalian circadian clock²⁴. We observed that both *DPP4* mRNA levels in IECs and sCD26/DPPIV concentrations fluctuated rhythmically, although *DPP4* mRNA levels were not significantly correlated with *Bmal1* (Fig. 3c, d).

We also examined *DPP4* mRNA expression in skin epithelial cells via analysis of the public Gene Expression Omnibus (GEO) dataset (GSE190035)²⁵. In wild-type (WT) mice, the *DPP4* mRNA levels in epithelial cells displayed a circadian rhythm, with the lowest expression at Zeitgeber time 12 (ZT12, dark onset) and the highest at ZT0 (Fig. 3e). In addition, correlation analysis of the dataset revealed a positive trend between *Bmal1* and *Dpp4* expression across time points ($r^2=0.142$, *P* = 0.070). However, in epithelial-specific *Bmal1* knockout (*Bmal1* Δ^{EC}) mice, this rhythmic expression of *DPP4* was absent (Fig. 3e). Collectively, these findings suggest that *DPP4* expression in epithelial cells may contribute to circadian fluctuations in sCD26/DPPIV levels.

DPPIV inhibitor administration mitigates aGVHD in mice

Next, we examined sCD26/DPPIV levels in mice after total body irradiation (TBI). Our recent study demonstrated that mice receiving stem cell infusion at ZT14 developed significantly less severe aGVHD than those infused at ZT5¹⁵. Correspondingly, sCD26/DPPIV levels were significantly lower at ZT14 than at ZT5. Furthermore, we observed that sCD26/DPPIV levels exhibited rhythmicity, with their levels gradually increasing during the active phase (Supplementary Fig. 3a). Consistent with this increasing trend during the active phase, in a major histocompatibility complex (MHC)-mismatched aGVHD mouse model, we found that aGVHD severity was greater in mice transplanted at ZT22 than in those transplanted at ZT14 (Supplementary Fig. 3b–e). These results indicate a positive correlation between pretransplant sCD26/DPPIV levels and aGVHD severity in mice.

To examine whether relatively high levels of sCD26/DPPIV may contribute to severe aGVHD, we blocked DPPIV activity with Sitagliptin, an FDA-approved DPPIV inhibitor, prior to transplantation in murine aGVHD models. We first employed a xenogeneic aGVHD mouse model in which NOD-scid IL2R $\gamma^{-/-}$ (NSG) mice were used. These mice were sublethally irradiated and then transplanted with thawed human cord blood. Mice scheduled for transplantation at ZT5 were treated with three doses of Sitagliptin before transplantation (Fig. 4a). Strikingly, prophylactic Sitagliptin administration significantly alleviated aGVHD severity and improved survival rates (Fig. 4b–d). No significant differences in body weight changes were observed between the two groups (Fig. 4e). Given that aGVHD arises from alloreactive donor T cells infiltrating and attacking host tissues, we further examined tissue pathology. Sitagliptin treatment significantly reduced tissue damage and T-cell infiltration—including both CD4⁺ and CD8⁺ T-cell subsets—in the liver, lung, and spleen, although no such effects were observed in the colon (Fig. 4f–k).

We also investigated the protective effect of Sitagliptin in the MHC-mismatched aGVHD mouse model (Supplementary Fig. 4a). Consistently, the administration of only two doses of Sitagliptin prior to transplantation significantly mitigated aGVHD severity, improved survival rates, and reduced tissue damage as well as lymphocyte infiltration in the ZT5 group (Supplementary Fig. 4b–k). However, Sitagliptin treatment failed to further improve survival or reduce aGVHD scores in the ZT14 group (Supplementary Fig. 4c–e).

Previous studies have shown that inhibition of CD26/DPPIV enhances SDF-1 α -mediated chemotaxis and promotes the engraftment of human hematopoietic stem/progenitor cells (HSPCs) in murine models and clinical settings^{26–29}. To determine whether Sitagliptin mitigates aGVHD by promoting the engraftment of HSPCs in our murine models, we evaluated peripheral white blood cell recovery and donor chimerism on day 14 posttransplantation. In both the xenogeneic and MHC-mismatched aGVHD models, no significant differences were observed between the Sitagliptin-treated and vehicle-

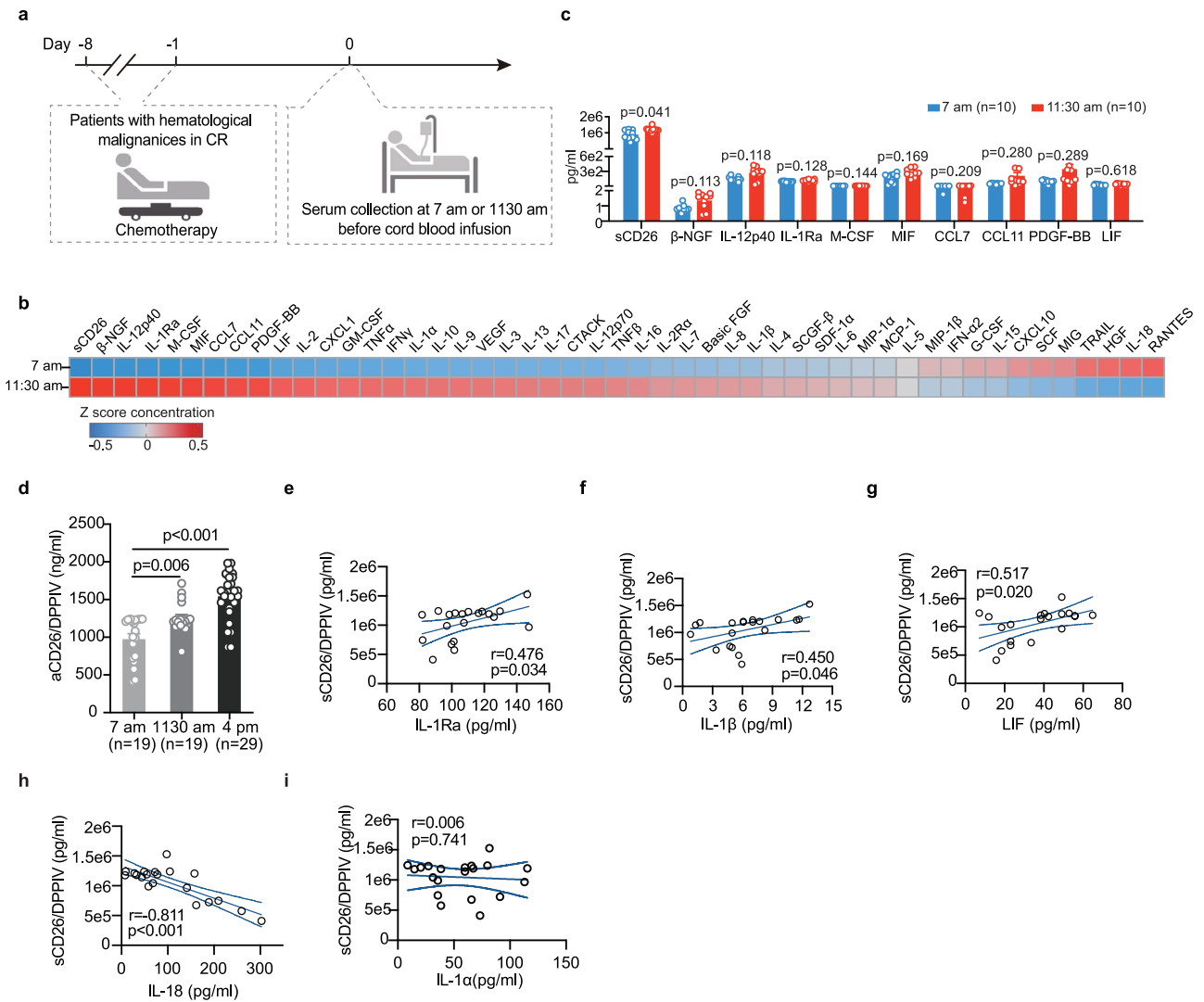


Fig. 2 | Circadian variation of sCD26/DPPIV levels and their association with pretransplant immune milieu. **a** Experimental design. Blood samples were collected at 7:00 am \pm 15 min ($n=10$) or 11:30 am \pm 15 min ($n=10$) from recipients with malignant hematological diseases in complete remission prior to cord blood infusion. **b**, **c** Serum concentrations of cytokines before cord blood infusion. Normalized z score (**b**) and absolute concentrations (**c**) of cytokines between 7:00 am and 11:30 am. The P values are two-sided and reported as exact values. **d** Absolute concentrations of soluble CD26/DPPIV in serum post-MAC. Blood samples were collected from recipients at 7:00 am \pm 15 min ($n=19$), 11:30 am \pm 15 min ($n=19$), or 4:00 pm \pm 15 min ($n=29$). **e–i** Associations between serum soluble CD26/DPPIV

(sCD26/DPPIV) levels and inflammatory cytokines before cord blood infusion on day 0. Pearson’s correlation coefficient (r) was calculated for the relationships between serum DPPIV levels and IL-1Ra (**e**) ($r=0.476$, $P=0.034$), IL-1 β (**f**) ($r=0.450$, $P=0.046$), LIF (**g**) ($r=0.517$, $P=0.020$), IL-18 (**h**) ($r=-0.811$, $P<0.001$) and IL-1 α (**i**) ($r=0.006$, $P=0.741$) concentrations. The P values are two-sided and reported as exact values. The data are presented as the means \pm SEMs and were analyzed by unpaired t test followed by Bonferroni-Dunn correction (**c**), one-way ANOVA with Bonferroni multiple comparisons (**d**) and Pearson’s correlation (**e–i**). Source data are provided as a Source Data file.

treated groups in terms of white blood cell (WBC) count, absolute neutrophil count (ANC), absolute lymphocyte count (ALC), or donor chimerism (Supplementary Fig. 4l–n). These results suggest that under high-dose cell transplantation conditions, the protective effect of Sitagliptin may not be due to improved hematopoietic engraftment and subsequent recovery. To assess whether Sitagliptin affects the function of HSPCs, we performed in vitro culture assays (Supplementary Fig. 5a). Compared with the PBS-treated group, Sitagliptin-treated group presented comparable percentages of viable CD34 $^{+}$ cells and colony-forming ability (Supplementary Fig. 5b–e), suggesting that Sitagliptin had no cytotoxic effects on HSPCs.

Recent studies have demonstrated that alloreactive CD8 $^{+}$ T cells in aGVHD encompass two key subpopulations: a TCF1 $^{+}$ PD-1 $^{+}$ progenitor-like subset with stem-like properties and a Tim-3 $^{+}$ PD-1 $^{+}$ effector-like subset with potent cytotoxic functions^{30,31}. Consistent with the reduced aGVHD severity, Sitagliptin-treated ZT5 recipients

exhibited significantly lower percentages of donor-derived CD8 $^{+}$ PD-1 $^{+}$ TCF1 $^{+}$ T cells in both peripheral blood and spleen on day 7 post transplantation compared to the control group (Supplementary Fig. 6). Given the established role of this subset as a proliferative progenitor population that gives rise to terminal effectors, our findings suggest that Sitagliptin can attenuate aGVHD by suppressing the early expansion of pathogenic progenitor CD8 $^{+}$ T cells.

sCD26/DPPIV promotes, while Sitagliptin inhibits, T-cell activation, proliferation, and differentiation

Alloreactive donor T cells from grafts are critical for the development of aGVHD¹. To explore the underlying mechanisms by which CD26/DPPIV and Sitagliptin regulate aGVHD progression, we cultured CD3 $^{+}$ cells from healthy donors with recombinant CD26/DPPIV protein (CD26 group), Sitagliptin (Sitagliptin group), or neither (control group). After 48 h of coculture, we performed RNA sequencing

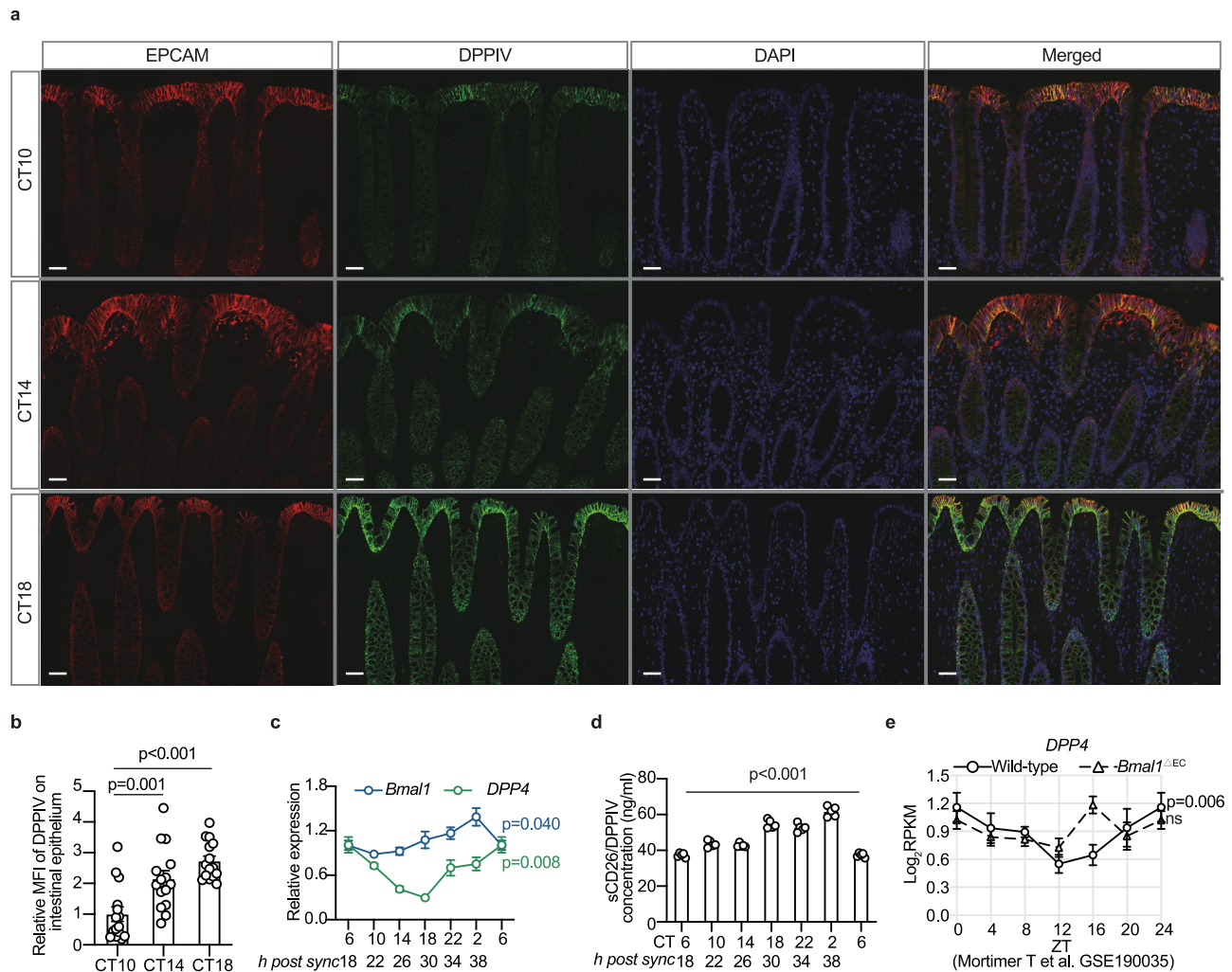


Fig. 3 | CD26/DPP4 levels on epithelial cells display circadian variation.

a, b Representative immunofluorescence images (**a**) and quantification (**b**) of CD26/DPP4 levels in intestinal epithelial cells from a healthy population at different times ($n = 3$ patients per group) ($P < 0.001$). Intestinal samples were collected at 10 am (CT10), 2 pm (CT14), and 6 pm (CT18). Scale bars, 50 μm . **c** *Bmal1* and *DPP4* expression in primary mouse epidermal cells postsynchronization in vitro ($n = 3$ biological replicates, each from an independent primary culture prepared and synchronized on separate days). The *Gapdh* gene was used as an internal control. The relative expression levels were computed via the $2^{-\Delta\text{ACT}}$ method. CT6 is double plotted. **d** The concentration of CD26/DPP4 in the supernatant of primary mouse

epidermal cells postsynchronization in vitro ($n = 3$ biological replicates, each from an independent primary culture prepared and synchronized on separate days) ($P < 0.001$). CT6 is double plotted. **e** Diurnal mRNA expression of *DPP4* in mouse epidermal cells. *Bmal1*^{EC}, epithelium cell-specific *Bmal1* knockout mice. Statistics were obtained from a publicly available dataset (GSE190035), with values representing the log₂-transformed mean RPKM from 4 biological replicates per time point. ZT0 is double plotted. The data are presented as the means \pm SEMs and were analyzed by one-way ANOVA with Bonferroni multiple comparisons (**b, d**) and JTK_Cycle²⁵ (**c, e**). Source data are provided as a Source Data file.

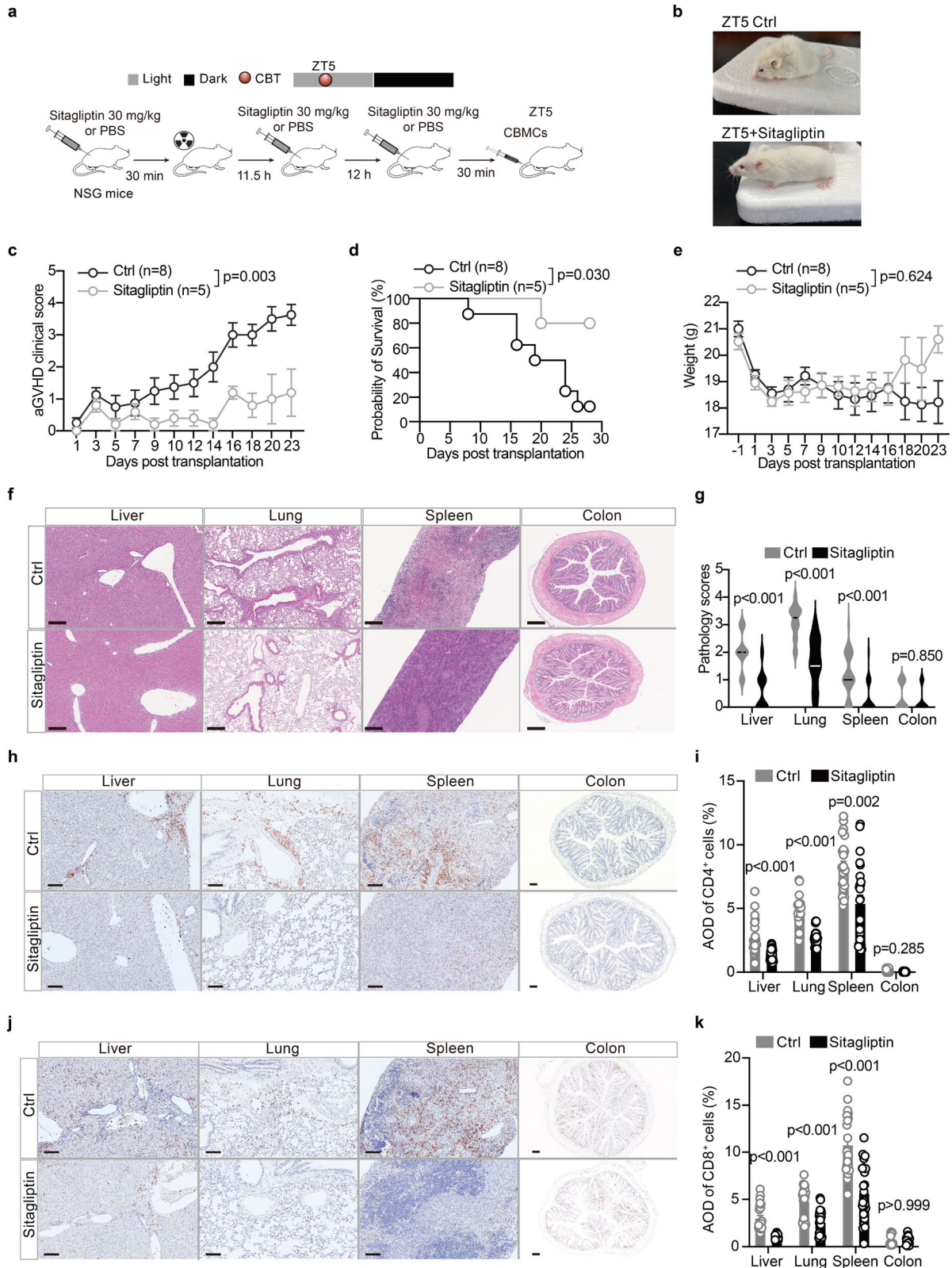
analysis of the sorted CD3⁺ cells, followed by flow cytometry detection at 72 h (Supplementary Fig. 7a and Supplementary Fig. 8).

Principal component analysis revealed a clear separation between the Sitagliptin group and the control group (Supplementary Fig. 7b). Differential gene analysis revealed approximately 2000 genes that were differentially expressed between the Sitagliptin and control groups (Supplementary Fig. 7c). In the Sitagliptin group, genes associated with resting naïve T cells and immune exhaustion (e.g., *CCR7*, *CXCR4*, *TIGIT*, *PDCD4*, and *TGFBRI*) were significantly upregulated compared with those in the control group. Conversely, T-cell markers (e.g., *CD4* and *CD8B2*) and genes related to cell activation, the cell cycle, and inflammatory factor secretion (e.g., *CDK2*, *CDKN3*, *CD38*, *IL17A*, *IL1R2*, *IRF8*, and *TNFRSF8*) were significantly lower in the Sitagliptin group (Supplementary Fig. 7d). Notably, genes linked to tumor killing, such as *GZMK* and *IFIT3*, were upregulated in the Sitagliptin group (Supplementary Fig. 7d). Gene Set Enrichment Analysis (GSEA) revealed that the Sitagliptin group presented significant upregulation

of pathways related to the negative regulation of the adaptive immune response, the negative regulation of T-cell-mediated immunity, and Treg differentiation, whereas oxidative phosphorylation was downregulated (Supplementary Fig. 7e).

Consistent with the RNA sequencing results, flow cytometry analysis revealed that Sitagliptin significantly suppressed T-cell activation (CD38⁺) (Supplementary Fig. 7f, g). Conversely, principal component analysis revealed no clear separation between the CD26 group and the control group (Supplementary Fig. 7b), and the administration of CD26/DPP4 did not increase CD38 expression on cultured T cells (Supplementary Fig. 7f, g), suggesting that sCD26/DPP4 may not have a direct effect on T-cell activation.

To determine whether Sitagliptin mitigates aGVHD by altering sCD26/DPP4 protein levels or enzymatic activity, we collected serum samples from lethally irradiated C57BL/6J mice 5 h post-irradiation at ZT5. These mice were treated with either Sitagliptin or vehicle prior to sample collection. DPP4 enzymatic activity was assessed via a



substrate hydrolysis-based luminescence assay, while sCD26/DPPIV protein levels were measured via ELISA (see “Methods”). We found that Sitagliptin treatment significantly reduced DPPIV enzymatic activity (Supplementary Fig. 9a), whereas sCD26/DPPIV protein levels were not affected (Supplementary Fig. 9b). Additionally, we measured serum IL-1 α levels in both vehicle- and Sitagliptin-treated mice prior to transplantation. No significant difference was observed between the groups

($P = 0.260$) (Supplementary Fig. 9c). Given that CD26/DPPIV functions as a potent costimulatory molecule on the T-cell membrane and that its enzymatic activity contributes to T-cell activation and proliferation^{21,23}, these results suggest that Sitagliptin likely impairs T-cell activation and mitigates aGVHD by directly inhibiting CD26/DPPIV enzymatic activity rather than by altering sCD26/DPPIV protein levels or serum IL-1 α levels.

Fig. 4 | Prophylaxis with Sitagliptin significantly ameliorates aGVHD and improves survival in mice. **a** Experimental design. Three doses of Sitagliptin (30 mg/kg, DPPIV inhibitor) or an equal volume of PBS were intraperitoneally given to ZT5 mice before human cord blood-derived mononuclear cells (CBMCs) infusions. **b** Representative images of PBS-treated (top) and Sitagliptin-treated (bottom) ZT5 recipients showing phenotypic differences on day 21 after CBT. **c–e** aGVHD scores (**c**, $P = 0.003$), survival rates (**d**, $P = 0.030$) and body weights (**e**, $P = 0.624$) of recipients posttransplantation ($n = 8$ mice for the control group; $n = 5$ for the Sitagliptin group). **f, g** Histopathologic analysis of liver, lung, spleen and colon sections on day 21 after CBT. Representative H&E-stained images (**f**) and quantification results (**g**) ($n = 24$ –30 images from 4–6 mice per group). Two-sided unpaired *t*-tests were used for comparisons. The exact *P* values were: $P < 0.001$ for

liver, lung, and spleen; $P = 0.850$ for colon. **h–k** The infiltration of CD4⁺ T cells and CD8⁺ T cells in liver, lung, spleen and colon sections on day 21 after transplantation. Representative immunohistochemistry images and quantification results of staining with anti-human CD4 (**h, i**) or CD8 (**j, k**) polyclonal antibodies ($n = 3$ mice per group; 24 fields of view were analyzed per organ). For CD4⁺ T cell infiltration, statistical comparisons yielded $P < 0.001$ for liver and lung, $P = 0.002$ for spleen, and $P = 0.285$ for colon; For CD8⁺ T cell infiltration, statistical comparisons yielded $P < 0.001$ for liver, lung and spleen, and $P > 0.999$ for colon. AOD, average optical density. Scale bars, 100 μm . The data are presented as the means \pm SEMs and were analyzed by unpaired *t* tests followed by Bonferroni-Dunn correction (**g, i and k**), two-way ANOVA followed by the Bonferroni post hoc correction (**c and e**), and the log-rank test (**d**). Source data are provided as a Source Data file.

Monocytes, the predominant APC population in the circulation system, play a pivotal role in initiating immune responses by processing and presenting antigens to T cells³². To investigate whether sCD26/DPPIV affects APC function, we cocultured peripheral blood mononuclear cells (PBMCs) from healthy donors with sCD26/DPPIV or Sitagliptin (Fig. 5a). We found that sCD26/DPPIV significantly upregulated CD86 expression on monocytes (CD14⁺) and slightly increased CD80 expression, although the latter did not reach statistical significance (Fig. 5b, c). In contrast, Sitagliptin had no notable effect on CD86 or CD80 expression on monocytes. Additionally, when APCs were present, sCD26/DPPIV significantly promoted T-cell proliferation (Ki-67), T-cell activation (CD38), and helper T-cell differentiation (IFN γ) (Fig. 5d–i), whereas Sitagliptin significantly inhibited these effects.

To further validate our findings in a TCR-dependent setting, we performed a mixed lymphocyte reaction (MLR) assay using human PBMCs (Fig. 6a). CellTrace™ Violet (CTV)-labeled responder PBMCs were cocultured with irradiated allogeneic PBMCs in the presence of recombinant sCD26/DPPIV or Sitagliptin. After 96 h, sCD26/DPPIV significantly enhanced CD4⁺ and CD8⁺ T cell proliferation and increased the proportion of IFN γ ⁺ cells in both subsets, whereas Sitagliptin markedly suppressed these responses (Fig. 6b–g). Interestingly, CD38 expression exhibited model-dependent dynamics: sCD26/DPPIV upregulated CD38 on CD4⁺ T cells in the MLR setting but had a minimal effect on CD8⁺ T cells, whereas PHA-L stimulation increased CD38 expression on both subsets. Sitagliptin consistently reduced CD38⁺ cell frequencies in both models (Fig. 6f, g). Collectively, these results suggest that sCD26/DPPIV may indirectly promote T-cell activation, proliferation, and differentiation by increasing the expression of the costimulatory molecules CD80 and CD86 on APCs, while Sitagliptin likely exerts direct effects on T cells.

Discussion

GVHD remains a major obstacle limiting the widespread use of allo-HSCT for treating both malignant and nonmalignant hematological disorders. Our previous study revealed that administering stem cell infusions before 2 pm significantly reduces the incidence and severity of aGVHD in allo-HSCT with freshly mobilized PBSCs from related donors¹⁵. The current study further demonstrated that early morning stem cell infusion substantially reduces the incidence of grade III–IV aGVHD and improves survival in patients who underwent UCBT with thawed cord blood from unrelated donors.

Interestingly, even within a relatively narrow morning time window, those who underwent UCBT earlier still exhibited a significantly lower severity of aGVHD. For PBSCT, the stem cell collection process typically takes at least 3–4 h, rendering early morning infusions challenging. In contrast, UCBT uses cryopreserved stem cells from public cord blood banks, enabling flexible scheduling of transplantation that can be conveniently adjusted according to actual clinical requirements. Our previous sensitivity analysis in the PBSCT cohort using multiple cutoff points (e.g., 1:00 pm, 2:00 pm) consistently demonstrated a lower incidence of aGVHD among patients infused earlier in

the day¹⁵. In the present UCBT cohort, absolute infusion time—when treated as a continuous variable—remained an independent risk factor for grade III–IV aGVHD in multivariate analysis. While the optimal transplantation window appears different between UCBT and PBSCT studies, both studies support that earlier graft infusion during the daytime is associated with reduced aGVHD risk.

To strengthen the mechanistic link between infusion timing and aGVHD severity, we comprehensively analyzed the circadian dynamics of preinfusion immune status. Notably, among all the cytokines examined, sCD26/DPPIV was the only factor that was significantly different between 7:00 am and 11:30 am, despite IL-1 α being implicated in our prior work¹⁵. We attribute this to the narrower sampling interval in the present cohort, which may have limited detection of circadian variation in IL-1 α levels. Additionally, we found no correlation between sCD26/DPPIV and IL-1 α concentrations in patient samples and that Sitagliptin treatment did not significantly alter systemic IL-1 α levels in mice. These data support the concept that recipient circadian rhythms shape the immune environment at the time of transplantation, thereby influencing donor T cell activation and subsequent aGVHD risk. Importantly, this effect is likely multifactorial rather than driven by a single cytokine. Therefore, IL-1 α and sCD26/DPPIV appear to contribute independently to this circadian modulation.

Complementing the circadian immune profiling, *in vitro* assays confirmed that sCD26/DPPIV enhances T cell proliferation, activation, and IFN γ production in both the CD4⁺ and CD8⁺ subsets, especially in the presence of antigen-presenting cells. We further validated these findings in a TCR-dependent MLR system in which recombinant sCD26/DPPIV significantly increased antigen-specific T cell responses, whereas Sitagliptin potently inhibited them. Previous animal studies have shown that the administration of a CD26 monoclonal antibody after transplantation decreases aGVHD severity and prolongs survival in mice³³. In our mouse models, short-course Sitagliptin administration significantly alleviated disease severity and prolonged survival in the ZT5 group but failed to further reduce aGVHD incidence in the ZT14 group, suggesting that DPPIV inhibition may provide limited additional benefit when transplant timing aligns with favorable circadian immune conditions.

The impact of DPPIV inhibition on hematopoietic stem and progenitor cell engraftment has been well documented. Broxmeyer et al. previously demonstrated that CD26/DPPIV inhibition enhances SDF-1 α -mediated chemotaxis and promotes human CD34⁺ cell engraftment in mice²⁶. Clinical studies have further suggested that oral Sitagliptin administration facilitates earlier neutrophil recovery in patients receiving UCBT²⁷. In our study, however, no significant differences in WBC counts, neutrophil or lymphocyte recovery, or donor chimerism were observed between the Sitagliptin-treated and control groups. This discrepancy may be explained by the high cell dose used in our murine models, which enables rapid hematopoietic reconstitution independent of DPPIV modulation. Importantly, these data indicate that the observed protective effects of Sitagliptin against aGVHD are unlikely to be driven by differences in engraftment efficiency. These

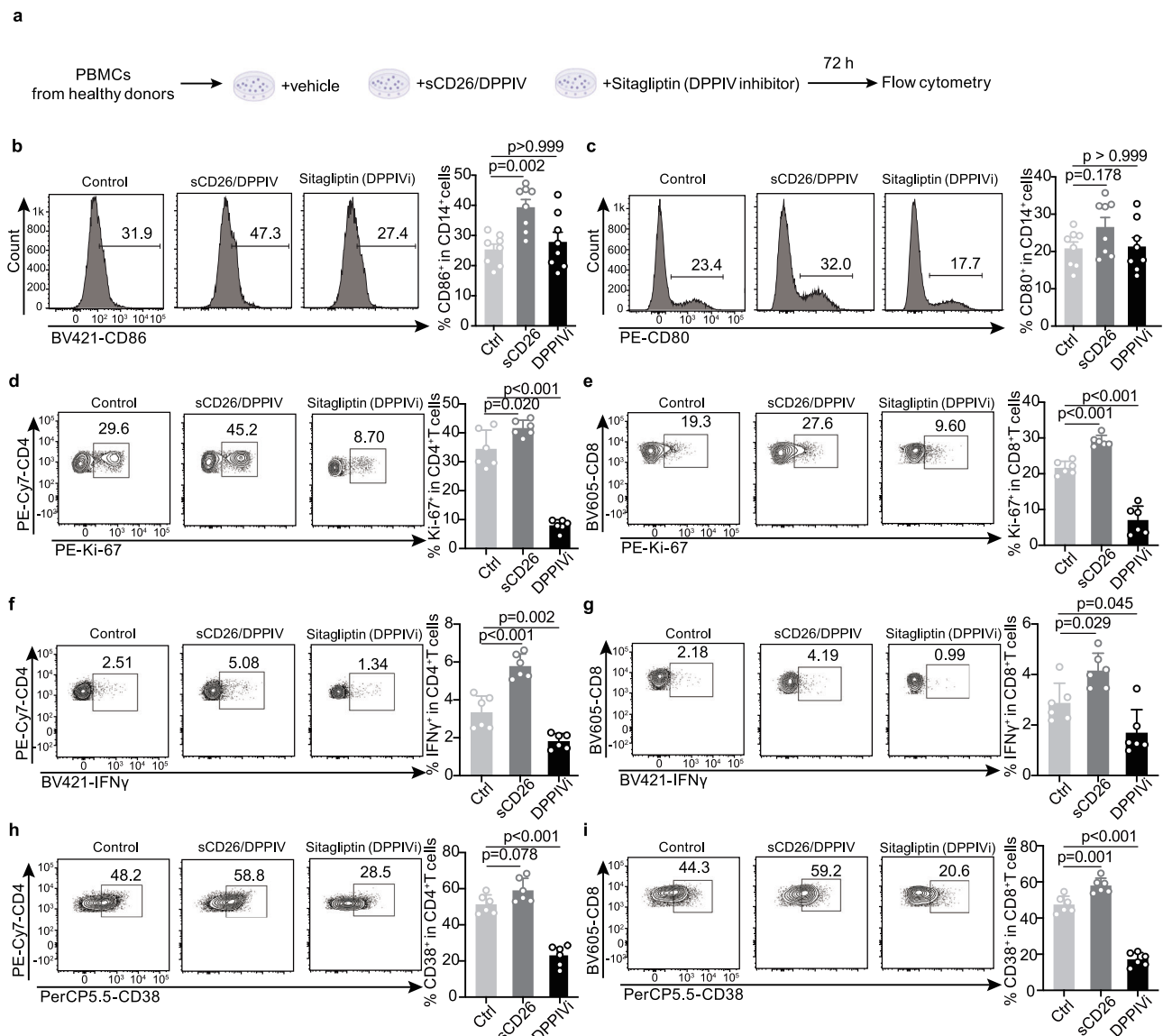


Fig. 5 | sCD26/DPPIV and Sitagliptin have opposite effects on the activation, proliferation, and differentiation of T cells. PBMCs from healthy donors were cultured with PHA-L (control group), PHA-L plus CD26/DPPIV (sCD26 group), or PHA-L plus Sitagliptin (DPPIV inhibitor, DPPIVi group) for 72 h. **a**, Experimental design. PBMCs from healthy donors were cultured with PHA-L (control group), PHA-L plus CD26/DPPIV (sCD26 group), or PHA-L plus Sitagliptin (DPPIV inhibitor, DPPIVi group) for 72 h. **b**, **c** Representative plots (left) and quantified percentages (right) of CD86⁺ (**b**) and CD80⁺ (**c**) CD14⁺ cells after 72 h of PBMCs coculture in

different groups (pooled data from 8 healthy donors across four independent experiments). **d–i** Representative plots (left) and quantified percentages (right) of Ki-67⁺, IFN γ ⁺, and CD38⁺ cells among CD4⁺ T cells (**d**, **f**, **h**) and CD8⁺ T cells (**e**, **g**, **i**) after 72 h of PBMCs coculture in different groups (pooled data from 6 healthy donors across three independent experiments). The data are presented as the means \pm SEMs and were analyzed by one-way ANOVA with the Bonferroni correction for multiple comparisons (**b–i**). All *P* values are two-sided and reported as exact values unless < 0.001 . Source data are provided as a Source Data file.

findings reinforce the interpretation that Sitagliptin primarily modulates posttransplant immune responses—particularly T cell activation—rather than altering graft kinetics. Similarly, in our clinical UCBT cohort, engraftment outcomes did not differ between the early-infusion and late-infusion groups. This finding further suggests that sCD26/DPPIV activity predominantly affects aGVHD through regulating immune responses rather than through enhancing hematopoietic recovery or changing graft kinetics.

A previous small-scale Phase II single-arm clinical trial (NCT02683525) revealed that 14 days of continuous Sitagliptin administration may improve aGVHD outcomes³⁴. Specifically, that trial revealed that patients who received Sitagliptin from day -1 to day +14 presented very low incidences of grade II-IV (5%) and grade III-IV (3%) aGVHD. In contrast to the continuous administration regimen, our study demonstrated that as few as 2-3 doses of Sitagliptin

administered prior to transplantation are sufficient to significantly mitigate aGVHD in mice. By reducing the need for long-term drug exposure, our approach may substantially minimize the potential risks of adverse effects typically associated with extended pharmacological interventions. Notably, the efficacy and safety of our abbreviated dosing strategy still need to be validated in well-designed large-scale prospective randomized clinical trials.

In summary, optimizing the timing of transplantation is crucial for preventing aGVHD and improving survival following the infusion of cryopreserved and thawed grafts. For patients whose transplantation timing cannot be optimized, DPPIV inhibitors such as Sitagliptin offer new strategies for aGVHD prevention. Future large-scale, prospective, multicenter, randomized clinical trials are needed to rigorously assess the efficacy and safety of these approaches, guiding clinical practice and improving allo-HSCT outcomes.

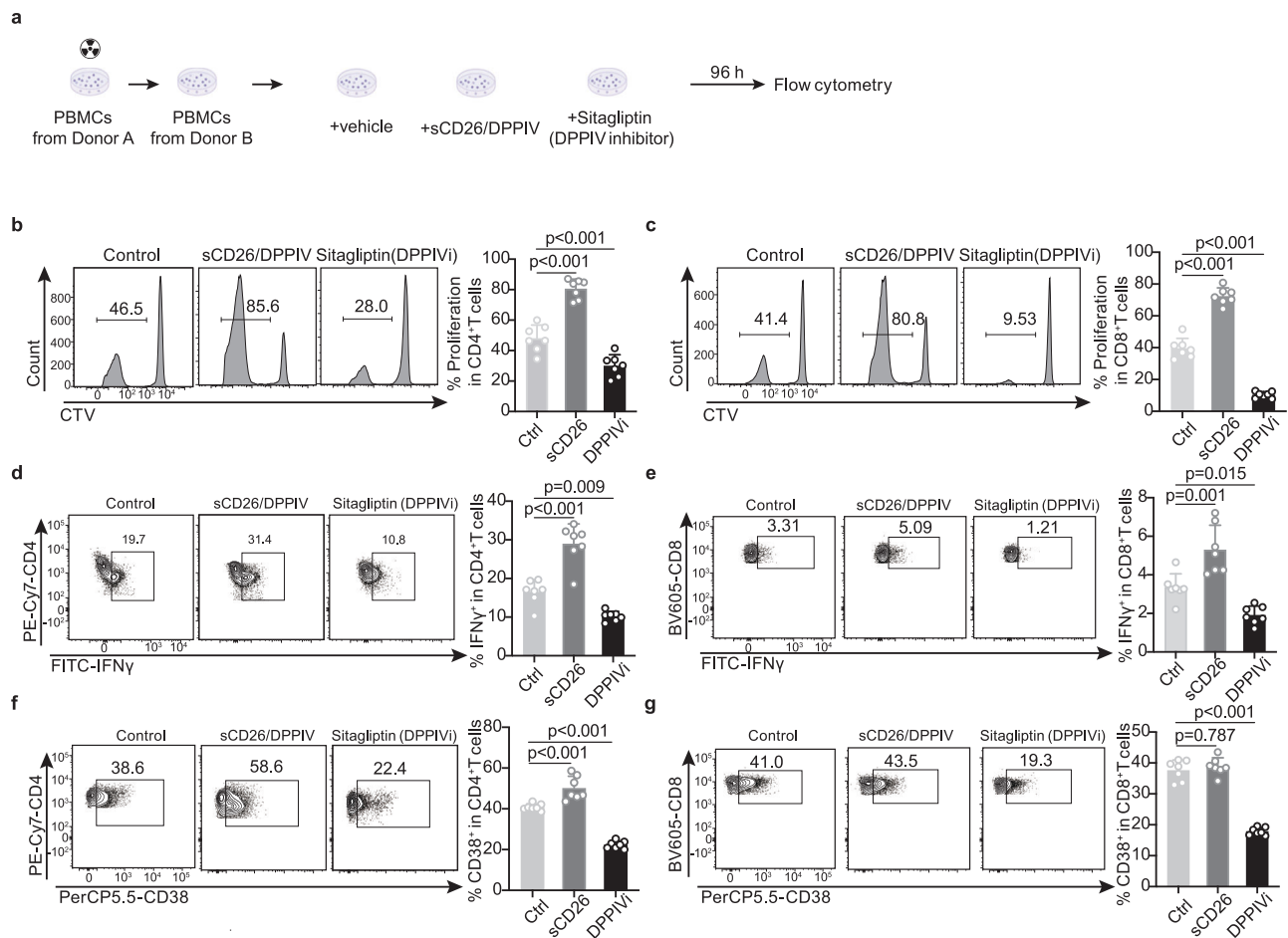


Fig. 6 | Effects of sCD26/DPPIV protein and Sitagliptin on allogeneic T cell responses in an MLR assay. **a** Experimental design. CellTrace™ Violet (CTV)-labeled human PBMCs were cocultured with irradiated allogeneic PBMCs in the presence of recombinant human sCD26/DPPIV protein (sCD26,1000 ng/ml) or Sitagliptin (200 μg/ml) for 96 h. **b, c** Representative plots (left) and quantified percentages (right) of cell proliferation in CD4⁺ (**b**) and CD8⁺ (**c**) T cells after 96 h of coculture. **d, e** Representative plots (left) and quantified percentages (right) of IFNγ

production in CD4⁺ (**d**) and CD8⁺ (**e**) T cells after 96 h of coculture.

f, g Representative plots (left) and quantified percentages (right) of CD38 expression in CD4⁺ (**f**) and CD8⁺ (**g**) T cells after 96 h of coculture. The data were pooled from three independent experiments. The data are presented as means ± SEMs. Statistical significance was determined by one-way ANOVA with Bonferroni correction (**b–g**). All *P* values are two-sided and reported as exact values unless <0.001. Source data are provided as a Source Data file.

Methods

Patient characteristics and cohort formation

Between January 2014 and December 2020, a total of 992 consecutive acute leukemia patients who underwent their first sUCBT at the First Affiliated Hospital of USTC were screened. All patients received cryopreserved cord blood sourced from unrelated donors, which was thawed prior to transplantation. Patients were excluded from the study on the basis of the following criteria: nonremission status ($n=193$), third or more complete remission ($n=245$), pretransplant minimal residual disease (MRD) positivity ($n=45$), incomplete clinical data ($n=62$) and infusion after 12 pm ($n=13$). After applying these exclusion criteria, the final cohort consisted of 434 MRD-negative patients. All surviving patients were followed up until December 31, 2023. The time of transplantation was defined as the initiation of cord blood infusion. This historical cohort study was approved by the Ethics Committee of the First Affiliated Hospital of the University of Science and Technology of China (REC reference: 2025/RE/154).

All human samples utilized in this study were collected with approval from the Ethics Committee of the First Affiliated Hospital of the University of Science and Technology of China (REC reference: 2023/KY/342). Written informed consent was obtained from each patient prior to participation.

Mice

NOD-scid IL2Ry^{-/-} (NSG), C57BL/6J (H2k^b), and BALB/c (H2k^d) mice were obtained from Shanghai Model Organisms Center, Inc., GemPharmatech Co., Ltd. (China), and Shanghai Silaike Experiment Animal Co., Ltd., respectively. The NSG and C57BL/6J mice were female, and the BALB/c mice were male. Prior to the initiation of the experimental procedures, the animals were acclimatized in a specific pathogen-free (SPF) facility for a minimum of one week.

The mice were housed under controlled environmental conditions, with a temperature range of 22–25 °C, relative humidity maintained between 40–70%, and a 12-h light/dark cycle (light from 8:00 am to 8:00 pm). The animals had ad libitum access to both water and a standard chow diet (SPF Rodent Feed; 4% fat, 18% protein, and 5% crude fiber; WQJX BIO-Technology, China).

All the mice used across the experimental groups were age-matched adult mice (9–12 weeks of age) to control for potential age-related immune variations. The care and use of the animals in this study were approved by the Institutional Animal Care and Use Committee (IACUC) of the University of Science and Technology of China (approval number: USTCACUC26110122040). All procedures adhered to the institutional guidelines and complied with relevant national regulations regarding animal experimentation.

Cord Blood Selection and HLA Typing

The selection of cord blood units and the human leukocyte antigen (HLA) typing process have been detailed in a previous publication³⁵. Briefly, both patients and cord blood units underwent high-resolution molecular HLA typing to identify matching alleles across the following 10 loci: HLA-A, HLA-B, HLA-C, HLA-DRB1, and HLA-DQB1. Cord blood units were obtained from the Chinese Cord Blood Bank. For transplantation, units were selected on the basis of a minimum 5/10 high-resolution allele match with the recipient. In addition, these units were required to meet the following criteria: total nucleated cells (TNCs) count of at least 3.0×10^7 cells per kilogram of recipient body weight and a minimum of 1.2×10^5 CD34⁺ cells per kilogram. All unrelated cord blood units used for transplantation were confirmed to be CMV-DNA negative. Moreover, all potential recipients were screened for anti-HLA antibodies within one month prior to UCBT. Cord blood units exhibiting donor-specific HLA antigens were excluded from use.

All patients underwent a myeloablative conditioning (MAC) regimen, with variations in protocols. The most common regimen, used for 391 patients, was based on busulfan (Bu) and cyclophosphamide (Cy). For this regimen, Bu was administered at 0.8 mg/kg every 6 h for 3 or 4 days, and Cy was given at 60 mg/kg per day for 2 days. Fludarabine (Flu) was added at a dose of 30 mg/m² daily for 4 days to all Bu/Cy patients. For 56 patients, an irradiation/Cy-based regimen was used. Four of these patients received total marrow irradiation (TMI) at a cumulative dose of 12 Gy, which was delivered in 4 fractions, whereas 52 patients received TBI at 12 Gy. Both TMI and TBI were combined with Cy at 60 mg/kg per day for 2 days. In this regimen, either fludarabine or cytarabine (Ara-C) was added, with Ara-C administered at 2 g/m² daily for 4 days.

GVHD prophylaxis involved the combination of CsA and MMF. CsA was initiated intravenously at 2.5–3 mg/kg/day starting on day –1, with the aim of maintaining blood concentrations between 200–300 ng/mL for at least one month. The route of administration was then switched to oral, with doses adjusted on the basis of GVHD progression or disease condition, maintaining a target trough concentration of 100–150 ng/mL for a minimum of four months. MMF was initiated orally at 25–30 mg/kg/day starting on day 1, with gradual dose reduction from day +21, and discontinuation after two months. No patients in either the earlier or later infusion groups discontinued CsA or MMF during the early posttransplant period because of drug-related toxicity or intolerance. All procedures followed standard UCBT protocols as outlined in prior studies³⁶.

Definitions

Disease risk was classified via the refined disease risk index (DRI-R) developed by Armand et al.¹⁹. Complete remission (CR) and complete remission with incomplete hematologic recovery (CRi) were determined on the basis of the criteria outlined in the National Comprehensive Cancer Network (NCCN) guidelines³⁷. All patients included in this study were MRD-negative prior to undergoing UCBT.

MRD status was assessed independently for AML and acute lymphoblastic leukemia (ALL) patients within 28 days prior to transplantation. Evaluation was performed via real-time quantitative polymerase chain reaction (RT-qPCR) with a sensitivity threshold of 10^{-4} ABL and/or multicolor flow cytometry (MFC) with a sensitivity threshold of 10^{-4} nucleated cells.

The definitions for graft function (GF), preengraftment syndrome (PES), acute graft-versus-host disease (aGVHD), and chronic graft-versus-host disease (cGVHD) were based on established criteria^{16,38,39}. The composite endpoint of graft-versus-host disease-free, relapse-free survival (GRFS) was defined as survival without the occurrence of grade III–IV aGVHD, cGVHD requiring systemic immunosuppression, or disease relapse.

aGVHD mouse models

BALB/c and C57BL/6J mice were used as donors and recipients, respectively, to establish an MHC-mismatched mouse model. Specifically, 9-week-old female C57BL/6J mice were subjected to a single 11 Gy dose of irradiation via a ¹³⁷Cs source irradiator. Following irradiation, these mice were intravenously injected with a mixture of 1×10^7 bone marrow cells and 6×10^7 splenocytes, which were harvested from 9-week-old male BALB/c mice 5–6 h after collection. To prevent infection, the recipient mice were given drinking water supplemented with gentamicin at a concentration of 320 mg/L, starting two days before irradiation and continuing until one week after transplantation.

A humanized GVHD model was developed using NSG mice and human mononuclear cells obtained from thawed cord blood. In this model, 9–10-week-old female NSG mice were irradiated with a single 3 Gy dose from a ¹³⁷Cs source irradiator. Twenty-four h post-irradiation, the mice were intravenously infused with 5×10^6 mononuclear cells from thawed human cord blood.

Donor cell collection

For the MHC-mismatched mouse model, donor cell collection began 3 h prior to transplantation. For recipient mice infused at ZT5, BALB/c donor mice were euthanized at approximately ZT2 to initiate cell collection. For recipient mice infused at ZT14, cell collection commenced when BALB/c donor mice were sacrificed at approximately ZT11.

Bone marrow cells were harvested from the femurs and tibias of the donor mice. These cells were subsequently resuspended in RPMI 1640 medium (C22400500BT, Gibco) supplemented with 2% fetal bovine serum (FBS; C04001-500, Biological Industries, Israel). Splenocytes were isolated by gently macerating the spleen through a 40 μ m mesh filter in RPMI 1640 medium containing 2% FBS. Erythrocytes were lysed by incubating the cell suspension in RBC Lysing Buffer (555899, BD Pharm Lyse) for 3 min at room temperature. The resulting cell suspension was passed through a 40 μ m strainer and washed twice with Dulbecco's Phosphate Buffered Saline (DPBS). The cell concentration was determined via a cell counter (Counter star, China), and the cells were then resuspended in 0.2 mL of DPBS per recipient for intravenous injection.

For the xenogeneic aGVHD model, cryopreserved human cord blood was obtained from the Shandong Cord Blood Bank (China). Mononuclear cells were isolated from the buffy coat via density gradient centrifugation. The isolated mononuclear cells were stored in liquid nitrogen and thawed for 2 hours prior to transplantation.

Cell culture assay

Fresh peripheral blood mononuclear cells (PBMCs) were isolated from healthy donors via Ficol-Paque Plus (P4350, Solarbio, China) density gradient centrifugation. The PBMCs were then cultured in RPMI-1640 medium (C22400500BT, Gibco) at a concentration of 1×10^6 cells per milliliter. To isolate CD3⁺ T cells, immunomagnetic depletion was performed via CD3 microbeads (130-050-101, Miltenyi Biotech) according to the manufacturer's protocol. The isolated CD3⁺ T cells were cultured in AIM-V medium (A3021002, Gibco) at a concentration of 2×10^5 cells/mL. For CD34⁺ cell isolation, immunomagnetic depletion was performed via CD34 microbeads (130-046-702, Miltenyi Biotech) following the recommended protocol. The isolated CD34⁺ cells were cultured in either StemSpan SFEM II medium (09655, STEMCELL Technologies) at 1×10^4 cells per milliliter or MethoCult™ H4435 enriched medium (04435, STEMCELL Technologies) at a density of 500 cells per well.

The PBMCs and CD3⁺ cell suspensions were supplemented with 100 IU/mL recombinant human interleukin-2 (IL-2; Jiangsu Kingsley Pharmaceutical Co., Ltd., China) and 10% fetal bovine serum (FBS;

VivaCell). All the cultures were incubated in a humidified incubator at 37 °C with 5% CO₂.

For *in vitro* assays, aliquots of PBMCs (1 × 10⁶ cells per milliliter) or CD3⁺ T cells (2 × 10⁵ cells per milliliter) were stimulated with 1.25 μg/mL phytohemagglutinin-L (PHA-L, 00-4977-93, eBioscience). In the experimental groups, recombinant human CD26/DPPIV protein (1000 ng/mL, 11244-SE, R&D Systems) or Sitagliptin phosphate monohydrate (DPPIV inhibitor, 200 μg/mL, S4002, Selleck) was added to the respective groups. The CD26/DPPIV protein was diluted with Tris-HCl (pH 8.0) (A2641, Promega) and Sitagliptin was diluted with PBS (BL310A, Biosharp).

After 8 h of incubation, the CD34⁺ cells were harvested, washed twice with PBS, and centrifuged at 400 × *g* for 5 min to remove residual medium. These cells were then prepared for apoptosis detection via flow cytometry. After 48 h of incubation, total RNA was extracted from the CD3⁺ T cells for RNA sequencing. After 72 h of incubation, the CD3⁺ T cells or PBMCs were washed and centrifuged for subsequent flow cytometry analysis. After 14 days of *in vitro* culture, the colony-forming ability of CD34⁺ cells was assessed by observing colony formation.

For the colony-forming assay, colony classification and enumeration were performed under an inverted microscope on the basis of morphological characteristics. Specifically, colony-forming unit-granulocyte (CFU-G) colonies appeared white; colony-forming unit-macrophage (CFU-M) colonies formed brown colonies with larger diameters than did CFU-G colonies. The colony-forming unit-granulocyte/macrophage (CFU-GM) colonies consisted of mixed granulocyte and macrophage colonies. The colony-forming unit-erythrocyte (CFU-E) presented as red or dark yellow colonies, whereas the colony-forming unit-granulocyte, erythrocyte, monocyte, and megakaryocyte (CFU-GEMM) represented mixed colonies comprising granulocytes, erythrocytes, monocytes, and megakaryocytes.

Mixed Lymphocyte Reaction (MLR)

To assess antigen-specific T cell responses, a mixed lymphocyte reaction (MLR) assay was performed by coculturing CellTrace™ Violet (C34557, Invitrogen)-labeled human PBMCs with irradiated (3000 cGy) allogeneic PBMCs at a responder-to-stimulator ratio of 2:1. Cultures were maintained for 96 h in the presence of either recombinant human CD26/DPPIV protein (1000 ng/mL; 11244-SE, R&D Systems) or Sitagliptin phosphate monohydrate (200 μg/mL; S4002, Selleck). After 96 h, the cells were harvested, washed, and subjected to flow cytometry.

RNA sequencing and data analysis

Total RNA was isolated from CD3⁺ cells via a TRIzol reagent kit (15596026CN; Invitrogen, Carlsbad, CA, USA) following the manufacturer's protocol. The quality of the extracted RNA was assessed via an Agilent 2100 Bioanalyzer (Agilent Technologies, Palo Alto, CA, USA) and further confirmed via RNase-free agarose gel electrophoresis. Eukaryotic mRNA was enriched from the total RNA via oligo(dT) beads. The enriched mRNA was then fragmented into smaller segments via fragmentation buffer. Following fragmentation, the mRNA was reverse-transcribed into complementary DNA (cDNA) with the NEB-Next Ultra RNA Library Prep Kit for Illumina (NEB #7530, New England Biolabs, Ipswich, MA, USA). The resulting double-stranded cDNA fragments underwent end repair, poly(A) tail addition, and ligation to Illumina sequencing adapters. The ligation reaction mixture was purified via AMPure XP beads (1.0X ratio), and PCR amplification was performed. The final cDNA library was sequenced on an Illumina NovaSeq 6000 system by Gene Denovo Biotechnology Co. (Guangzhou, China).

Principal component analysis (PCA) was performed via the R package *gmodels*, available at <http://www.r-project.org/>. RNA differential expression analysis between two distinct groups was conducted via DESeq2 software (R package, version 1.20.0)⁴⁰, whereas comparisons between two individual samples were analyzed via

edgeR⁴¹. Differentially expressed genes were identified using an adjusted *P* value of less than 0.05 and an absolute fold change greater than 1.5 as the significance thresholds. The final *P* values were adjusted using the Benjamini-Hochberg method to control the false discovery rate.

Flow cytometry

To assess the effect of Sitagliptin on the differentiation of donor-derived CD8⁺ T cells *in vivo*, peripheral blood and spleens were harvested from recipient mice on day 7 post-transplantation and dissociated through a 40-μm cell strainer in RPMI 1640 medium containing 20 mg/mL BSA (Thermo Fisher Scientific). After red blood cell lysis with RBC Lysis Buffer and washing with FACS buffer, cells were blocked using anti-mouse CD16/CD32 antibody (1 μg/mL, BE0307, BioXcell) for 10 min at 4 °C to prevent nonspecific binding. Surface staining was then performed with the following fluorochrome-conjugated antibodies: Fixable Viability Dye (FVD, eFluor 506, eBioscience) to exclude dead cells, BV661 anti-H2k^d (1 μg/mL, BioLegend), APC-Cy7 anti-CD45 (1 μg/mL, BioLegend), PE-Cy5 anti-CD3 (1 μg/mL, BioLegend), SB702 anti-CD4 (1 μg/mL, RM4-5), PE-Cy5.5 anti-CD8 (1 μg/mL, 53-6.7), PE-Cy7 anti-PD-1 (1 μg/mL, RMP1-30) and APC anti-Tim-3 (1 μg/mL, RMT3-23). Intracellular staining was performed after fixation and permeabilization using the Foxp3/Transcription Factor Staining Buffer Set (eBioscience), followed by staining with PE anti-TCF1 (1 μg/mL, C63D9).

To assess the antigen presentation ability of monocytes and the function of T cells in cell culture assays, the following antibodies were used: AF700 anti-CD45 (1 μg/mL, 2D1), APC-H7 anti-CD3 (1 μg/mL, SK7), BV650 anti-CD56 (1 μg/mL, NCAM16.2), PE-Cy7 anti-CD4 (1 μg/mL, RPA-T4), BV605 anti-CD8 (1 μg/mL, SK1), PerCP5.5 anti-CD38 (1 μg/mL, Ab90), BV510 anti-CD14 (1 μg/mL, 63D3), PE anti-CD80 (1 μg/mL, W17149D), and BV421 anti-CD86 (1 μg/mL, FUN-1). All antibodies have been validated by the manufacturers or in previous studies^{15,30}. The cells were incubated with these antibodies for 30 minutes at 4 °C. For the intracellular staining of IFN γ and Ki-67, the cells were fixed and permeabilized with Foxp3/Transcription Factor Staining Buffer (00-5523-00, eBioscience) according to the manufacturer's instructions. The cells were then stained with BV421 anti-IFN γ (1 μg/mL, B27) and PE anti-Ki-67 (1 μg/mL, Ki-67). A fixable viability dye (FVD, eFluor 520, 65-0867-14, eBioscience) was used to exclude dead cells from the viable cell population.

To evaluate the cytotoxic effects of Sitagliptin on CD34⁺ cells, the cells were resuspended in Annexin V binding buffer and labeled with APC-Annexin V (550474, BD) and DAPI solution (564907, BD) following the manufacturer's protocols. Flow cytometry was performed 15 minutes post-staining. The cells were gated on the basis of Annexin V and DAPI expression: viable cells (DAPI⁻ Annexin V⁻), early apoptotic cells (DAPI⁻ Annexin V⁺), late apoptotic cells (DAPI⁺ Annexin V⁺), and necrotic cells (DAPI⁺ Annexin V⁻).

Detailed information on the antibodies used is provided in Supplementary Data 3. The expression of TCF1, Tim-3, CD80, CD86, CD38, IFN- γ , and Ki-67 was assessed via the fluorescence minus one (FMO) gating strategy. The gating strategies are detailed in Supplementary Fig. 6a and Supplementary Fig. 8. The cells were resuspended in 200 μL of FACS buffer and analyzed via FACS Aria II (BD Biosciences) and FlowJo v10 software (FlowJo, Ashland, OR, USA).

Quantitative polymerase chain reaction

Total RNA was extracted using chloroform and isopropanol. Following extraction, reverse transcription was performed via the SuperScript™ III First-Strand Synthesis System for RT-PCR (18080-051, Invitrogen) according to the manufacturer's protocol. PCR amplification was initiated with an initial denaturation step at 95 °C for 2 min. This was followed by 40 cycles, each consisting of denaturation at 95 °C for 15 seconds, annealing at 55 °C for 15 seconds, and extension at 72 °C for

1 min. The *Gapdh* gene was used as an internal control. Relative expression levels were calculated via the $2^{-\Delta\Delta CT}$ method. The sequences of the primers used in this study are provided in Supplementary Table 2.

aGVHD scoring

Following transplantation, recipient animals were monitored daily for survival, and the appearance of aGVHD symptoms was assessed twice weekly. The severity of aGVHD was evaluated by scoring key parameters, including weight loss, activity level, posture (manifested as hunching), and fur ruffling. Each parameter was assigned a score ranging from 0 to 2: 0 indicated a normal condition, 1 signified a mildly abnormal condition, and 2 represented a severely abnormal condition. The overall aGVHD clinical score was calculated by summing the scores for all four parameters. Mice that reached a moribund state or had a cumulative aGVHD clinical score greater than 5 were humanely euthanized.

Measurement of cytokine levels

Patient serum was isolated from residual peripheral blood samples collected at 7:00 am \pm 15 min and 11:30 am \pm 15 min following the completion of the myeloablative conditioning regimen at the First Affiliated Hospital of USTC. This collection was conducted with approval from the Ethics Committee of the First Affiliated Hospital of USTC (REC reference: 2023/KY/342). Immediately after collection, the samples were stored at 4 °C and processed within 4 h. The serum was separated via centrifugation at $1000 \times g$ for 5 min at 4 °C, transferred to cryovials, and stored at -80 °C. All the serum samples were analyzed within 1 to 4 months of storage, and each batch of assays included both early- and late-infusion group samples to control for potential batch effects. For mouse serum samples, cytokine levels were measured via a mouse inflammation panel (740150, Biolegend) according to the manufacturer's instructions. Human serum cytokine concentrations were assessed via the Bio-Plex Pro Human Cytokine Screening Panel (12007283, Bio-Rad), with analysis conducted via LabEx (Shanghai). Data analysis was performed via FCAP Array Software (version 3.0, BD Biosciences), the Luminex X-200 system (Luminex) and Milliplex Analyst software (version 5.1).

Histopathologic analysis of GVHD target organs

Histopathological analysis of GVHD target organs was conducted following a previously described methodology¹⁵. Briefly, formalin-fixed and paraffin-embedded (FFPE) sections of the primary target organs for GVHD, namely, the skin, liver, colon, lung, and spleen, were stained with hematoxylin and eosin (HE). Following staining, histopathological examination was performed. The severity of GVHD in these tissues was evaluated via a semiquantitative scoring system^{42,43}, with scoring conducted in a blinded manner.

Immunohistochemistry

IHC staining of formalin-fixed, paraffin-embedded (FFPE) tissue sections was performed as previously described¹⁵. Briefly, the tissue sections were deparaffinized and rehydrated, followed by antigen retrieval by boiling the slides in EDTA Antigen Retrieval Solution (pH 9.0) (G1203, Servicebio, China). Immunostaining was carried out via the following antibodies: anti-human CD4 (ab133616, Abcam, dilution 1:500), anti-human CD8 (ZA-0508, ZSGB-BIO, dilution 1:100), anti-mouse CD4 (25229S, CST, dilution 1:100), and anti-mouse CD8 (A23305PM, ABclonal, dilution 1:300). Images were captured and stitched using an automated slide scanner (Pannoramic M, 3DHISTECH). All the samples were scored in a double-blinded manner, with eight randomly selected fields scored for each sample. The relative intensity of CD4 and CD8 staining in each organ is expressed as the average optical density (AOD) percentage and was analyzed via ImageJ software.

Mouse intestinal epithelial cell culture and synchronization

Mouse primary intestinal epithelial cells were obtained from Wuhan Procell Co., Ltd. (CP-M030). The primary cells were cultured in complete media (Procell CM-M030).

Cell synchronization was achieved via the use of horse serum, as previously described¹². Briefly, mouse intestinal epithelial cells were harvested and seeded into 6-well plates in complete medium. An equal volume of prewarmed horse serum (16050122, Gibco) was added to the wells for serum shock. After a 2-h incubation at 37 °C in a 5% CO₂ atmosphere, the cells were washed and resuspended in fresh complete medium.

CD26/DPPIV activity and concentration detection

Serum samples collected from patients and mice at various time points were analyzed for DPPIV activity via the DPPIV-Glo™ Protease Assay Kit (G8350, Promega). The concentration was detected with the ELISA assay (DC260B, R&D Systems). For enzymatic activity measurements, recombinant human CD26/DPPIV protein (R&D) was serially diluted in Tris-HCl buffer (pH 8.0, Promega) to generate a standard curve. Patient and mouse serum samples were diluted 1:1000 in Tris-HCl buffer (Promega) and assayed according to the manufacturer's instructions. For protein concentration measurements, the serum samples were diluted 1:1000 and analyzed using the ELISA kit following the manufacturer's protocol. For in vitro culture supernatants from mouse primary intestinal epithelial cells, the culture media were diluted 100-fold before concentration measurement.

IF staining assays

Intestinal biopsy samples from healthy human were collected with approval from the Ethics Committee of the First Affiliated Hospital of the University of Science and Technology of China (REC reference: 2023/KY/342). Frozen tissue sections were subjected to immunofluorescence (IF) staining for EpCAM and CD26/DPPIV. Antigen retrieval was performed by boiling the sections in EDTA Antigen Retrieval Solution (pH 8.0) (G1206, Servicebio, China). The sections were then blocked with 3% bovine serum albumin (BSA) blocking buffer for 30 minutes. Following blocking, the sections were incubated overnight at 4 °C with an anti-CD26/DPPIV antibody (ab215711, Abcam, diluted 1:2000) and an anti-EpCAM antibody (ab213500, Abcam, diluted 1:10000). After incubation, the slides were incubated for 50 min with an HRP-conjugated goat anti-mouse IgG (H + L) secondary antibody (GB23301, Servicebio, diluted 1:250). This was followed by a 10-min incubation with FITC-tyramide (G1222, Servicebio, diluted 1:500) and CY3-tyramide (G1223, Servicebio, diluted 1:500). Images were captured and stitched via an automated slide scanner (NanoZoomer S60, HAMAMATSU). The mean fluorescence intensity (MFI) of CD26/DPPIV was quantified via ImageJ software. For each sample, the data points represent the integrated intensity from 3–5 randomly selected fields and are normalized to the average intensity of the CT10 group. Three patients were analyzed per group.

In vivo inhibitor treatment

To inhibit DPPIV activity in ZT5 recipient mice, the animals were intraperitoneally injected with 30 mg/kg of Sitagliptin phosphate monohydrate (S4002, Selleck) or an equal volume of PBS as indicated.

Statistical analysis

Two-tailed *t* tests or Mann-Whitney U tests were used to compare continuous variables. For categorical data, chi-square tests or Fisher's exact tests were applied. The ordinal data were analyzed using the Cochran-Armitage trend test. For multiple comparisons, one-way or two-way analysis of variance (ANOVA) was performed, followed by Bonferroni post hoc correction.

In a competing-risk framework, with death as a competing event, the cumulative incidences of engraftment, aGVHD, cGVHD, TRM, and

relapse were estimated. Comparisons among these cumulative incidences were performed via Gray's test⁴⁴. TRM was defined as death occurring without disease relapse, with relapse considered a competing risk factor for TRM. The Kaplan-Meier method, combined with the log-rank test, was used to assess the probabilities of overall survival (OS), disease-free survival (DFS), and graft-versus-host disease-free, relapse-free survival (GRFS).

Multivariate analyses for aGVHD and TRM were conducted using a Fine-Gray proportional hazards regression model, whereas Cox proportional hazards regression models were used for OS, DFS, and GRFS^{45,46}. The evaluated variables included absolute infusion time, patient age, sex (male vs. female), refined disease risk index (DRI-R; low vs. intermediate vs. high), complete remission status (CR vs. CRI), donor/recipient sex combination (female donor to male recipient vs. others), ABO compatibility (identical vs. minor incompatibility vs. major incompatibility vs. bidirectional incompatibility), high-resolution HLA compatibility (10 loci), infused total nucleated cells (TNCs) and CD34⁺ cell counts, and conditioning regimen (irradiation-based vs. Bu-based). DRI-R, ABO compatibility, and HLA compatibility were treated as ordinal variables. Independent risk factors were identified via the stepwise selection method on the basis of the *P* value.

All the statistical analyses were performed via R software, version 4.2.2 (R Foundation for Statistical Computing, Vienna, Austria), and GraphPad Prism 9.0 (GraphPad Software, CA, USA). The data are presented as the means ± standard errors of the mean (SEMs), and results with a two-sided *P* value < 0.05 were considered statistically significant.

Reporting summary

Further information on research design is available in the Nature Portfolio Reporting Summary linked to this article.

Data availability

Source Data are provided with this paper. The RNA expression datasets generated in this study are available in the Gene Expression Omnibus database under accession code [GSE294787](https://www.ncbi.nlm.nih.gov/geo/query/acc.cgi?acc=GSE294787). The RNA expression data used in this study are available in the Gene Expression Omnibus database under accession code [GSE190035](https://www.ncbi.nlm.nih.gov/geo/query/acc.cgi?acc=GSE190035). Any additional information required to reanalyze the data reported in this paper is available from the lead contact upon request. Source data are provided with this paper.

Code availability

This paper does not report any original code.

References

- Ferrara, J. L., Levine, J. E., Reddy, P. & Holler, E. Graft-versus-host disease. *Lancet* **373**, 1550–1561 (2009).
- Zeiser, R. & Blazar, B. R. Acute graft-versus-host disease - biologic process, prevention, and therapy. *N. Engl. J. Med.* **377**, 2167–2179 (2017).
- Malard, F., Holler, E., Sandmaier, B. M., Huang, H. & Mohty, M. Acute graft-versus-host disease. *Nat. Rev. Dis. Prim.* **9**, 27 (2023).
- Hexner, E. O. & DeFilipp, Z. Update in GVHD prophylaxis: novel pharmacologic and graft manipulation strategies. *Am. J. Hematol.* **100**, 30–39 (2025).
- Scheiermann, C., Kunisaki, Y. & Frenette, P. S. Circadian control of the immune system. *Nat. Rev. Immunol.* **13**, 190–198 (2013).
- Wang, C., Lutes, L. K., Barnoud, C. & Scheiermann, C. The circadian immune system. *Sci. Immunol.* **7**, eabm2465 (2022).
- Druzd, D. et al. Lymphocyte Circadian Clocks Control Lymph Node Trafficking and Adaptive Immune Responses. *Immunity* **46**, 120–132 (2017).
- Suzuki, K., Hayano, Y., Nakai, A., Furuta, F. & Noda, M. Adrenergic control of the adaptive immune response by diurnal lymphocyte recirculation through lymph nodes. *J. Exp. Med.* **213**, 2567–2574 (2016).
- Gibbs, J. et al. An epithelial circadian clock controls pulmonary inflammation and glucocorticoid action. *Nat. Med.* **20**, 919–926 (2014).
- Ince, L. M. et al. Influence of circadian clocks on adaptive immunity and vaccination responses. *Nat. Commun.* **14**, 476 (2023).
- Wang, C. et al. Dendritic cells direct circadian anti-tumour immune responses. *Nature* **614**, 136–143 (2023).
- Wang, C. et al. Circadian tumor infiltration and function of CD8(+) T cells dictate immunotherapy efficacy. *Cell* **187**, 2690–2702 e2617 (2024).
- Fortin, B. M. et al. Circadian control of tumor immunosuppression affects efficacy of immune checkpoint blockade. *Nat. Immunol.* **25**, 1257–1269 (2024).
- Karaboue, A. et al. Why does circadian timing of administration matter for immune checkpoint inhibitors' efficacy? *Br. J. Cancer* **131**, 783–796 (2024).
- Hou, Y. et al. Optimizing stem cell infusion timing in the prevention of acute graft-versus-host disease. *Cell* **27**, 3030–3044 (2025).
- Harris, A. C. et al. International, Multicenter Standardization of Acute Graft-versus-Host Disease Clinical Data Collection: A Report from the Mount Sinai Acute GVHD International Consortium. *Biol. Blood Marrow Transpl.* **22**, 4–10 (2016).
- Jagasia, M. et al. Risk factors for acute GVHD and survival after hematopoietic cell transplantation. *Blood* **119**, 296–307 (2012).
- Flowers, M. E. et al. Comparative analysis of risk factors for acute graft-versus-host disease and for chronic graft-versus-host disease according to National Institutes of Health consensus criteria. *Blood* **117**, 3214–3219 (2011).
- Armand, P. et al. Validation and refinement of the Disease Risk Index for allogeneic stem cell transplantation. *Blood* **123**, 3664–3671 (2014).
- von Bonin, A., Huhn, J. & Fleischer, B. Dipeptidyl-peptidase IV/CD26 on T cells: analysis of an alternative T-cell activation pathway. *Immunol. Rev.* **161**, 43–53 (1998).
- Morimoto, C. & Schlossman, S. F. The structure and function of CD26 in the T-cell immune response. *Immunol. Rev.* **161**, 55–70 (1998).
- Mertens, R. T. et al. A metabolic switch orchestrated by IL-18 and the cyclic dinucleotide cGAMP programs intestinal tolerance. *Immunity* **57**, 2077–2094 e2012 (2024).
- Ohnuma, K. et al. Role of CD26/dipeptidyl peptidase IV in human T cell activation and function. *Front Biosci.* **13**, 2299–2310 (2008).
- Abe, Y. O. et al. Rhythmic transcription of *Bmal1* stabilizes the circadian timekeeping system in mammals. *Nat. Commun.* **13**, 4652 (2022).
- Mortimer, T. et al. The epidermal circadian clock integrates and subverts brain signals to guarantee skin homeostasis. *Cell Stem Cell* **31**, 834–849 e834 (2024).
- Broxmeyer, H. E., Capitano, M., Campbell, T. B., Hangoc, G. & Cooper, S. Modulation of Hematopoietic Chemokine Effects In Vitro and In Vivo by DPP-4/CD26. *Stem Cells Dev.* **25**, 575–585 (2016).
- Farag, S. S. et al. In vivo DPP-4 inhibition to enhance engraftment of single-unit cord blood transplants in adults with hematological malignancies. *Stem Cells Dev.* **22**, 1007–1015 (2013).
- Christopherson, K. W. 2nd, Paganessi, L. A., Napier, S. & Porecha, N. K. CD26 inhibition on CD34+ or lineage- human umbilical cord blood donor hematopoietic stem cells/hematopoietic progenitor cells improves long-term engraftment into NOD/SCID/Beta2null immunodeficient mice. *Stem Cells Dev.* **16**, 355–360 (2007).
- Christopherson, K. W. 2nd, Hangoc, G., Mantel, C. R. & Broxmeyer, H. E. Modulation of hematopoietic stem cell homing and engraftment by CD26. *Science* **305**, 1000–1003 (2004).

30. Lee, S. et al. Defining a TCF1-expressing progenitor allogeneic CD8(+) T cell subset in acute graft-versus-host disease. *Nat. Commun.* **14**, 5869 (2023).
31. Quann, K. et al. The role of TCF-1+CD8+ exhausted progenitors and TCF-1 in graft-versus-host responses. *JCI Insight* **10**, e181568 (2025).
32. Jakubzick, C. V., Randolph, G. J. & Henson, P. M. Monocyte differentiation and antigen-presenting functions. *Nat. Rev. Immunol.* **17**, 349–362 (2017).
33. Hatano, R. et al. Prevention of acute graft-versus-host disease by humanized anti-CD26 monoclonal antibody. *Br. J. Haematol.* **162**, 263–277 (2013).
34. Farag, S. S. et al. Dipeptidyl peptidase 4 inhibition for prophylaxis of acute graft-versus-host disease. *N. Engl. J. Med.* **384**, 11–19 (2021).
35. Wu, Y. et al. Ruxolitinib plus basiliximab therapy for steroid-refractory acute graft-versus-host disease in unrelated cord blood transplantation: a large-scale study. *Transpl. Cell Ther.* **30**, 916 e911–916.e912 (2024).
36. Wu, Y. et al. The clinical influence of preformed nonspecific anti-HLA antibodies on single-unit umbilical cord blood transplantation in patients with haematological malignancies. *Br. J. Haematol.* **198**, e63–e66 (2022).
37. Pollyea, D. A. et al. NCCN Guidelines Insights: Acute Myeloid Leukemia, Version 2.2021. *J. Natl. Compr. Canc Netw.* **19**, 16–27 (2021).
38. Park, M. et al. Pre-engraftment syndrome after unrelated cord blood transplantation: a predictor of engraftment and acute graft-versus-host disease. *Biol. Blood Marrow Transpl.* **19**, 640–646 (2013).
39. Jagasia, M. H. et al. National institutes of health consensus development project on criteria for clinical trials in chronic graft-versus-host disease: I. the 2014 diagnosis and staging working group report. *Biol. Blood Marrow Transpl.* **21**, 389–401 e381 (2015).
40. Love, M. I., Huber, W. & Anders, S. Moderated estimation of fold change and dispersion for RNA-seq data with DESeq2. *Genome Biol.* **15**, 550 (2014).
41. Robinson, M. D., McCarthy, D. J. & Smyth, G. K. edgeR: a Bioconductor package for differential expression analysis of digital gene expression data. *Bioinformatics* **26**, 139–140 (2010).
42. Blazar, B. R. et al. Engraftment of severe combined immune deficient mice receiving allogeneic bone marrow via In utero or post-natal transfer. *Blood* **92**, 3949–3959 (1998).
43. Kaplan, D. H. et al. Target antigens determine graft-versus-host disease phenotype. *J. Immunol.* **173**, 5467–5475 (2004).
44. Klein, J. P., Rizzo, J. D., Zhang, M. J. & Keiding, N. Statistical methods for the analysis and presentation of the results of bone marrow transplants. Part I: unadjusted analysis. *Bone Marrow Transpl.* **28**, 909–915 (2001).
45. Klein, J. P., Rizzo, J. D., Zhang, M. J. & Keiding, N. Statistical methods for the analysis and presentation of the results of bone marrow transplants. Part 2: Regression modeling. *Bone Marrow Transpl.* **28**, 1001–1011 (2001).
46. Fine, J. P. & Gray, R. J. A proportional hazards model for the sub-distribution of a competing risk. *J. Am. Stat. Assoc.* **94**, 496–509 (1999).

Acknowledgements

We thank the animal facility and flow cytometry facility at USTC for their technical support. Xiaoyu Zhu is supported by grants from the National Natural Science Foundation of China (U23A20453, 82270223), the USTC Research Funds of the Double First-Class Initiative (YD9110002047), the Anhui Provincial Department of Education Scientific Research Project (2023AH010079) and the Anhui Provincial Natural Science Foundation

(2308085J09). Cheng Zhan is supported by grants from the National Natural Science Foundation of China (32525034, 82495183, 32271063), the Research Funds of the Center for Advanced Interdisciplinary Science and Biomedicine of IHM (QYPY20220018), and the National Science and Technology Innovation 2030 Major Project of China (2021ZD0203900). Yiwen Hou is supported by grants from the USTC Research Funds of the Double First-Class Initiative (YD9990006006) and the National Natural Science Foundation of China (32400831).

Author contributions

X.Y.Z. (Xiaoyu Zhu), C.Z. (Cheng Zhan), and B.L.T. (Baolin Tang) conceived and supervised the study. Y.W. (Yue Wu) performed the retrospective clinical analysis and in vitro cell culture assays and drafted the manuscript. Y.W. and Y.W.H. (Yiwen Hou) developed the aGVHD mouse model and performed histopathological evaluation. J.L.Z. (Jialin Zhou) and L.W. (Liang Wang) contributed to cytokine measurements. W.W.W. (Weiwei Wu) and Y.W. conducted the data analysis. D.Y.W. (Dongyao Wang), K.D.S. (Kaidi Song), G.Y.S. (Guangyu Sun), A.J.H. (Aijie Huang), M.J.T. (Meijuan Tu), and L.H. (Lu Huang) provided clinical or laboratory data. The manuscript was revised by X.Y.Z. and C.Z. All authors reviewed, modified, and approved the final version of the manuscript.

Competing interests

The authors declare no competing interests.

Additional information

Supplementary information The online version contains supplementary material available at <https://doi.org/10.1038/s41467-026-68958-4>.

Correspondence and requests for materials should be addressed to Baolin Tang, Cheng Zhan or Xiaoyu Zhu.

Peer review information *Nature Communications* thanks Satoshi Takahashi, and the other, anonymous, reviewer(s) for their contribution to the peer review of this work. A peer review file is available.

Reprints and permissions information is available at <http://www.nature.com/reprints>

Publisher's note Springer Nature remains neutral with regard to jurisdictional claims in published maps and institutional affiliations.

Open Access This article is licensed under a Creative Commons Attribution-NonCommercial-NoDerivatives 4.0 International License, which permits any non-commercial use, sharing, distribution and reproduction in any medium or format, as long as you give appropriate credit to the original author(s) and the source, provide a link to the Creative Commons licence, and indicate if you modified the licensed material. You do not have permission under this licence to share adapted material derived from this article or parts of it. The images or other third party material in this article are included in the article's Creative Commons licence, unless indicated otherwise in a credit line to the material. If material is not included in the article's Creative Commons licence and your intended use is not permitted by statutory regulation or exceeds the permitted use, you will need to obtain permission directly from the copyright holder. To view a copy of this licence, visit <http://creativecommons.org/licenses/by-nc-nd/4.0/>.

© The Author(s) 2026